sciendo
Austrian Journal of Earth Sciences | Vienna | 2022 | Volume 115 | 74 - 99 | DOI: 10.17738/ajes.2022.0004

Stratigraphic architecture of a mixed clastic-carbonate succession and $^{87}Sr/^{86}Sr$-based chronostratigraphy along the margin of a synorogenic extensional basin (Hochmoos Formation, upper Santonian, Northern Calcareous Alps)

Kevin Kearney[1]*, Michael Wagreich[1], Diethard Sanders[2]
[1)] Department of Geology, University of Vienna, A-1090 Vienna, Austria.
[2)] Institute of Geology, University of Innsbruck, Innrain 52, A-6020 Innsbruck, Austria.
[*)] Corresponding author, kevin.kearney@outlook.com

KEYWORDS
Stratigraphy, Gosau Group, Hochmoos Formation, carbonate rocks, Late Cretaceous, Santonian

Abstract

The Gosau Group (Turonian to Ypresian) of the Eastern Alps is a synorogenic wedge-top succession that accumulated in active depocenters in an oblique-convergent plate tectonic setting. Due to high morphological differentiation of depocenters by tectonism, the Gosau Group displays a wide range of facies as well as marked facies heteropy and thickness variations over short lateral distances. In the area of the locations Gosau and Russbach, the Hochmoos Formation along the SE basin margin near Gosauschmied comprises coastal to shallow-marine deposits and small rudist bioconstructions and was investigated by way of field mapping, profile descriptions, microfacies analysis, isotope measurements and assessment of fossil content.

Strontium isotope ratios ($^{87}Sr/^{86}Sr$) from 0.707485 (oldest) to 0.707549 (youngest) indicate a latest Santonian age, with the youngest parts of the Hochmoos Formation possibly extending into the Campanian. On the west side of the study area, the succession of lithologies and fossil content record transgression of a fan-delta to marginal-marine environment (lowstand to transgressive systems tract), followed by shallow neritic deposition (part of the transgressive systems tract) and, finally, by progradational stacking of limestone beds in the highstand systems tract, culminating in growth of rudist thickets in an inner shelf and partially protected 'lagoonal' milieu. Eventually, at the inception of the following falling stage systems tract, input of large clasts of Dachstein Limestone, quartz and chert record a recurrence of the subaqueous part of a fan-delta. On the east side of the study area, a preponderance of rudist-clastic limestones over a few rudist biostromes preserved *in situ* indicate a normal-marine environment punctuated by high-energy events, such as storms or tsunami. The scarcity of benthic foraminifera and the presence of only isolated specimens of colonial corals underscore a habitat with a calcarenitic substrate frequently shifted by currents. Several lines of evidence indicate that the western part of the study area was more proximal relative to the eastern one. With a maximum thickness of 68 m, the Hochmoos Formation at Gosauschmied is slightly thicker and more distal than outcrops located nearer to the basin margin and farther towards the SE (Schmiedsippl, Katzhofgraben), but significantly thinner than the nearly 300 m at Gosau Pass-Gschütt, or the thickness of 170 m observed in the area of Rigaus-Abtenau farther in the West. These thickness variations are interpreted as a result of extensional syndepositional tectonism. At Gosauschmied, the vertical arrangement of facies records a cycle of relative sea-level change that may have been tectonically enhanced.

1. Introduction

The Upper Cretaceous and Paleogene sediments of the Gosau Group are among the most significant in the Northern Calcareous Alps (NCA) and are widely distributed throughout the NCA (Fig. 1). Beginning in the Late Cretaceous, the NCA Gosau Group sediments were deposited unconformably upon the Upper Austroalpine nappe complex (Wagreich and Faupl, 1994). One of the most extensive and most notable occurrences of Gosau Group sediments in the NCA can be found in the Gosau basin at the border area of Upper Austria and Salzburg, where most of the type localities for the Gosau Group are located. The Gosau basin covers an area of approximately 80 km^2 with a width of roughly 8 km and a length of about 10 km and straddles the Salzburg-Upper Austrian border in the Gosau-Russbach-Pass Gschütt area (Wagreich and Decker, 2001). The Gosau Group

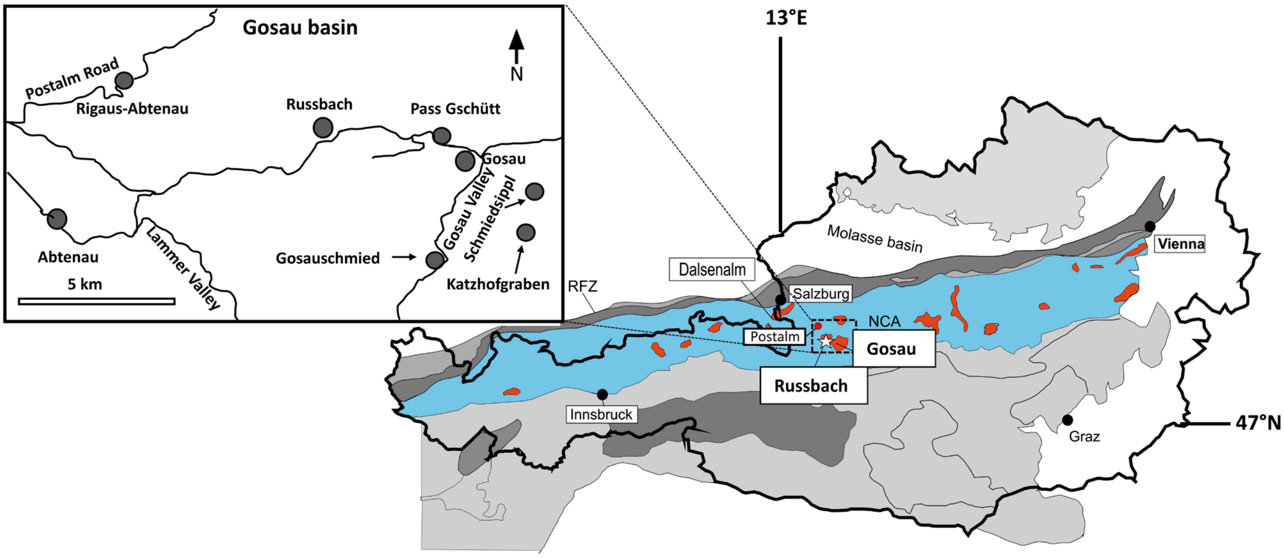

Figure 1: Geological sketch map of the Austrian Eastern Alps including Gosau Group locations (red) in the Northern Calcareous Alps of Austria (Modified from Wolfgring et al., 2018) and the position of Gosau, Russbach and Postalm in the Gosau basin; the Northern Calcareous Alps (NCA, blue). Dark grey = Penninic Units (including RFZ = Rhenodanubian Flysch Zone); medium gray = other Austroalpine units; white = Cenozoic basins. Insert to the left shows key occurences of the Hochmoos Formation in the Gosau basin and the position of Gosauschmied (adapted from Wagreich et al., 2010).

sediments range temporally from ca. 90 Ma to 50 Ma and are divided into two distinct subgroups: the Lower Gosau Subgroup (LGS), ranging from the upper Turonian to the lower Campanian, and the Upper Gosau Subgroup (UGS), ranging diachronously from the lower Campanian to the Ypresian (Wagreich, 2003). The Upper Cretaceous Lower Gosau Subgroup (LGS) consists of alluvial/terrestrial and transgressive shallow-marine sediments that reach a total thickness of about 1000 m (Sanders and Höfling, 2000) in the Gosau basin. These are primarily found in an E-W-oriented section of the basin stretching from Gosau Vordertal across the Gschütt Pass and over to Russbach in Salzburg (Wagreich, 1988). Although LGS outcrops are more widespread in the northern part of the Gosau basin, there are also significant LGS occurrences in its southern part: the Hochmoos Formation (upper Santonian) at Gosauschmied south of Gosau Hintertal, as well as the Untersberg Formation (lower Campanian) further south/southeast of this area, and at Schmiedsippl at the east margin of the basin (Wagreich and Neuhuber, 2005). In addition, a relatively small occurrence of the Bibereck Formation (lower Campanian) can be found directly north and west of the main studied outcrops of the Hochmoos Formation at Gosauschmied (095 St. Wolfgang im Salzkammergut 1:50 000, GBA, 1982), with a second, smaller occurrence transgressing onto the Untersberg Formation, which was studied extensively by Trenkwalder (1999). To date, however, no exhaustive stratigraphic analysis of the Hochmoos Formation in Gosauschmied has been undertaken.

The objectives of this study are threefold:

1. To undertake a thorough stratigraphic analysis of three selected outcrops (designated W1, W2 and E1) in the Hochmoos Formation in Gosauschmied.
2. To investigate the entire study area in this part of the Gosau basin and determine holistic facies development and types from base to top in the various sections.
3. To correlate the different outcrops to each other and develop deposition scenarios that take into account lithology, structural data, tectonics, isotope data and overall macro- and microfossil content. To this end, comparisons will be made with other occurrences of the Hochmoos Formation in the Gosau basin and to similar LGS structures throughout the NCA to correlate lithofacies, fossil assemblages and possible deposition scenarios.

2. Geological setting

The Northern Calcareous Alps (NCA) comprise a significant portion of the Upper Austroalpine nappe stack. The Eastern Alps, characterized by the Austroalpine tectonostratigraphic domain, originated in the northwestern Tethys paleogeographic belt upon repeated convergence between the European and the African plate and the intercalated Austroalpine and Adriatic microplate, respectively (Wagreich et al., 2008). During the Late Cretaceous, the accretionary wedge of the NCA was sheared off from its basement and entered a phase of tectonic subsidence that, apart from one constrained, but significant period of uplift, continued at varying rates into the Eocene. During the Late Cretaceous, the NCA deformational belt was located at approximately 32° N according to paleomagnetic measurements (Wagreich and Faupl, 1994). This is roughly 1800 km to the south of their current position at about 47° N.

The subsidence of the N/NW-moving accretionary wedge led to deposition of the Gosau sediments on the

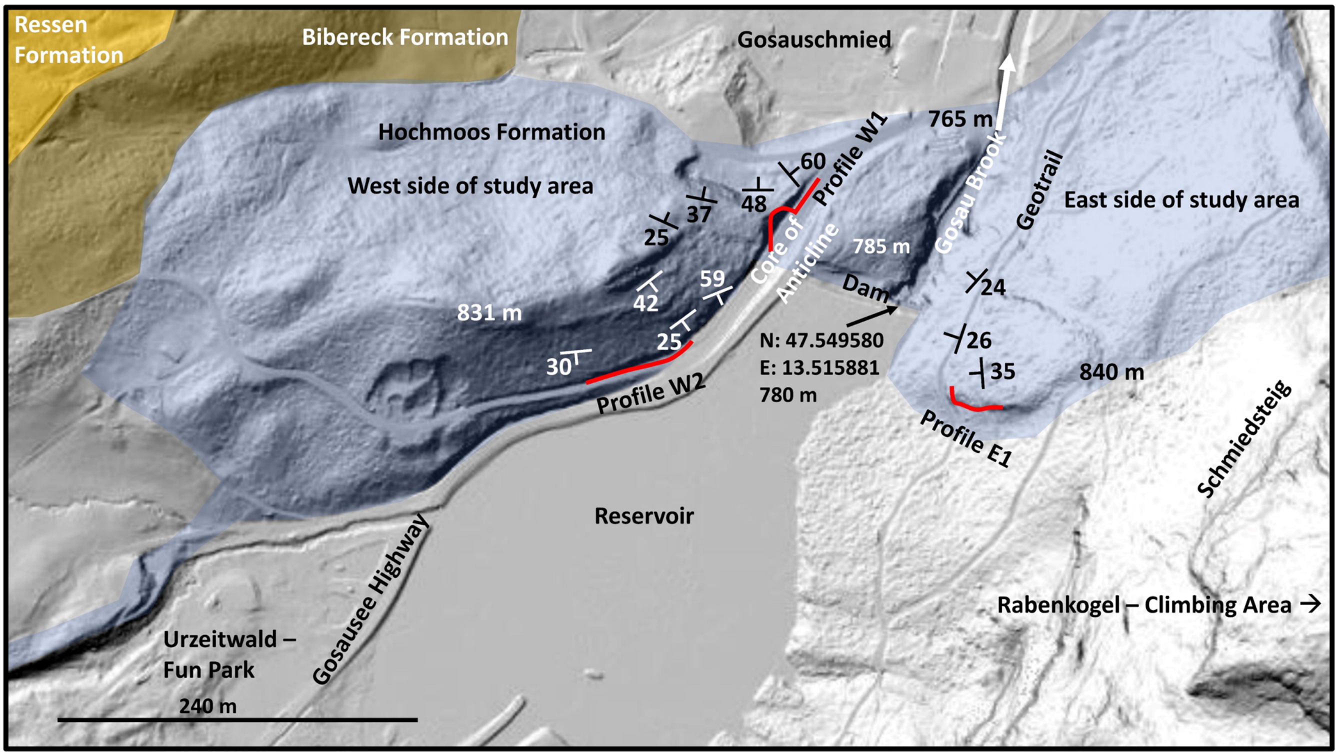

Figure 2: Overview of study area in Gosauschmied, indicating key formations of the Gosau Group and the extent of the Hochmoos Formation. Included are key structures, places, topography, strike/dip measurements and elevation. Morphologically and structurally, the west and east sides of the area dip toward the brook running N-NE through the valley and northward into the Gosau basin. The reservoir is at around 780 m. (Digitales Oberösterreichisches Raum-Informations-System [DORIS] – accessed on 10 May 2021.)

submerging flanks of what, in the Late Cretaceous, were structural island arcs of primarily Triassic origin in the Western Tethys. Today's Dachstein Massif, upon which the Gosau sediments in the Gosau basin are unconformably overlain, was part of such a Triassic structural island arc in the NCA deformational belt during the Late Cretaceous. The subsidence rates and sedimentation rates during the Turonian to late Santonian varied considerably from those of the Campanian to the Eocene (Wagreich and Faupl, 1994).

These varying subsidence rates account for the starkly different nature of the sediments in the Lower Gosau Subgroup (LGS) and the Upper Gosau Subgroup (UGS). In the LGS, which ranges temporally from the late Turonian to the early Campanian, subsidence rates were comparatively modest and produced alluvial/terrestrial and shallow marine carbonate sediments containing a wealth of Upper Cretaceous fossils. Towards the end of the Santonian and the beginning of the Campanian, a relatively brief period of tectonic uplift occurred, resulting in marine regression and subsequent subaerial erosive activity in the uppermost LGS sediments (Wagreich, 1988). The UGS, subsequent to this brief uplift, is marked by precipitous subsidence, which, in turn, led to marine depths in the bathyal to abyssal range, descending even below the Calcite Compensation Depth (Wagreich and Faupl, 1994; Wagreich, 2003). Consequently, UGS formations are largely void of macrofossil content and consist of deep-water clastics and pelagic marls overlying the LGS unconformably (Wagreich and Faupl, 1994). In total, Gosau Group sediments attain local thicknesses of up to 2500 m, as in the area around the village of Gosau.

The study area is located in the southern portion of the Gosau basin and includes the entire Hochmoos Formation at Gosauschmied and peripheral areas of adjacent formations, most notably the Bibereck Formation to the north and west of the Hochmoos Formation. Outcrops of the Hochmoos Formation comprise total dimensions of approximately 1 km W to E and a half kilometer N to S, extending from the Geotrail in the west (N 47.550556, E 13.508395) to the top of the Rabenkogel near the rock-climbing area in the east (N 47.550047, E 13.521416), and from the settlement at Gosauschmied in the north (N 47.551089, E 13.515548) to the amusement park Urzeitwald in the south (N 47.547496, E 13.511068) (see Fig. 2). The Gosausee highway cuts diagonally through the area; and its renovation and expansion in the 1980s directly produced many significant outcrops of the Hochmoos Formation. The water reservoir behind the Gosauschmied power station is also a prominent feature of the landscape and, together with the Gosau brook that issues from it and flows N/NE, divides the Hochmoos Formation at Gosauschmied into two separate outcrop areas, west and east. The Hochmoos Formation is situated on two limestone/carbonate elevations that dip toward the Gosau brook flowing through the valley and the reservoir behind the dam of the hydroelectric power station (see strike/dip symbols in Fig. 2).

3. Material and methods

3.1 Stratigraphic survey work and profile description

The field work took place from May to November, 2019. Three outcrops belonging to the Hochmoos Formation at Gosauschmied (designated W1, W2 and E1) were selected for detailed stratigraphic analysis (Fig. 2). An anticline structure to the south of profile W1 as well as outcrops surrounding W1, W2 and E1 were also examined to achieve a holistic stratigraphic overview of the entire Hochmoos Formation in the study area.

3.2 Sample and thin section preparation and analysis

A total of 113 thin sections (4 x 4 cm) were prepared from the collected samples and scrutinized under light and polarization microscopes. A total of 41 samples were collected for use in isotope analysis.

A marl microfossil sample taken from the stratigraphically oldest interval in the study area was ground up and dissolved in a 1:1 H_2O_2 solution for three days. Two fractions were sieved from the resulting slurry at 0.5 mm and 0.125 mm, then dried overnight in an 80°C kiln. In addition, 2 nannofossil suspension slides were prepared for calcareous nannofossil biostratigraphy evaluation, using scratched sediment powder suspended with distilled water in a beaker. After 2h, the superfluent was removed, and a new suspension was spread on a glass cover plate, dried and fixed on a glass slide. Slides were examined qualitatively using a polarised light (100x oil immersion objective) Zeiss microscope.

3.3 Chronostratigraphy and stable isotope analysis

A total of 41 bulk carbonate samples were selected and prepared for carbon ($\delta^{13}C$) and oxygen ($\delta^{18}O$) isotope measurement. Great care was taken to ensure that no material was taken from secondary diagenetic sections of the rock. Adequate sample amounts (about 100 µg) were pulverized from the rock specimens using a traditional power drill. The actual measurement was undertaken using a ThermoFinnigan Delta$_{plus}$XL mass spectrometer equipped with a Gas-Bench II at the Institute of Geology, University of Innsbruck, following the procedure described in Spötl and Vennemann (2003) (Wolfgring et al., 2018). The results were calibrated against NBS 19, CO1 and CO8 standard reference materials and are reported on the VPDB (Vienna Pee Dee Belemnite) scale.

Regarding $^{87}Sr/^{86}Sr$ ratio measurements, three samples were taken from rudist shells in profile E1. An additional two measurements were made of a rudist sample from profile W2 and a limestone sample at the top of the ridge behind profiles W1 and W2. Hence, a total of five $^{87}Sr/^{86}Sr$ measurements were obtained for correlating the ages of the separate outcrops. The shells were analyzed to ensure no diagenetic material corrupted the primary calcite of the fossils, and 200–300 µg of powdered material was extracted using a dentist's power drill. Strontium was separated by standard ion exchange chromatography. Samples were measured on a Triton mass spectrometer at the geochronological laboratory of the Department of Lithospheric Research, University of Vienna (see also Wolfgring et al., 2018). The precision of the measurements is in the range of +/- 0.000005; and raw ratios were adjusted according to a NIST 987 standard value of 0.710248 as recommended by McArthur et al. (2001).

3.4 Classification of mixed carbonate-siliciclastic compositions

The Lower Gosau Subgroup displays a wide and highly variable range of compositions of clastic sediments and sediment textures. Because of this variability, and because the relative amounts of sediment components were not quantified in every case (except for biogenic limestones), we have adopted a simplified scheme in this study that was derived from the classifications of Folk (1954, 1980) and Pettijohn et al. (1973) and has proven to be of excellent utility (Sanders, 1998) (see Tab. 1).

4. Results

4.1 Facies distribution

The stratigraphic survey, sample collection and microfacies analysis in the Hochmoos Formation at Gosauschmied led to the definition of six facies types (Figs 3 and 4). These are summarized in Table 2 and characterized as follows:

Type F1: mixed sandy/carbonate-lithic wacke and pebbly wacke with low fossil content and small to medium-sized terrigenous clasts (carbonate lithoclasts, quartz, chert), less structurally competent than either F2 or F3 with medium-gray/brown color. This facies is typical of the core of the anticline (beds 1–7 in profile W1).

Type F2: peloidal packstone to grainstone with limited to zero content in bioclasts, very competent and of medium-gray color. This facies comprises the beds 14–24 in profile W1.

Type F3: bioclastic rudstone to floatstone to packstone with many large bioclasts of rudists and corals, less dense than Type F2, but still competent with a medium to light gray color. This facies is found in profile E1 and the area surrounding it.

Type F4: This limestone facies is transitional between Type F3 and Type F5: in profile W2, the initial two beds are rich in bioclasts and constitute rudstones to floatstones, with micrite as the primary matrix component and sparite infilling the bioclasts. Higher up-section, the content in bioclasts decreases, while that of peloids increases; in addition, clay content decreases ('upward cleaning'). Carbonate lithoclasts also increase in number as the facies transitions to F5.

Type F5: Peloidal limestone with carbonate lithoclasts. Very similar to facies type F2, but with a higher content of sand- to pebble-sized lithoclasts – mainly clasts of Dachstein Limestone, quartz and chert; varying fossil content that decreases in higher beds; very competent with medium- to dark-gray color.

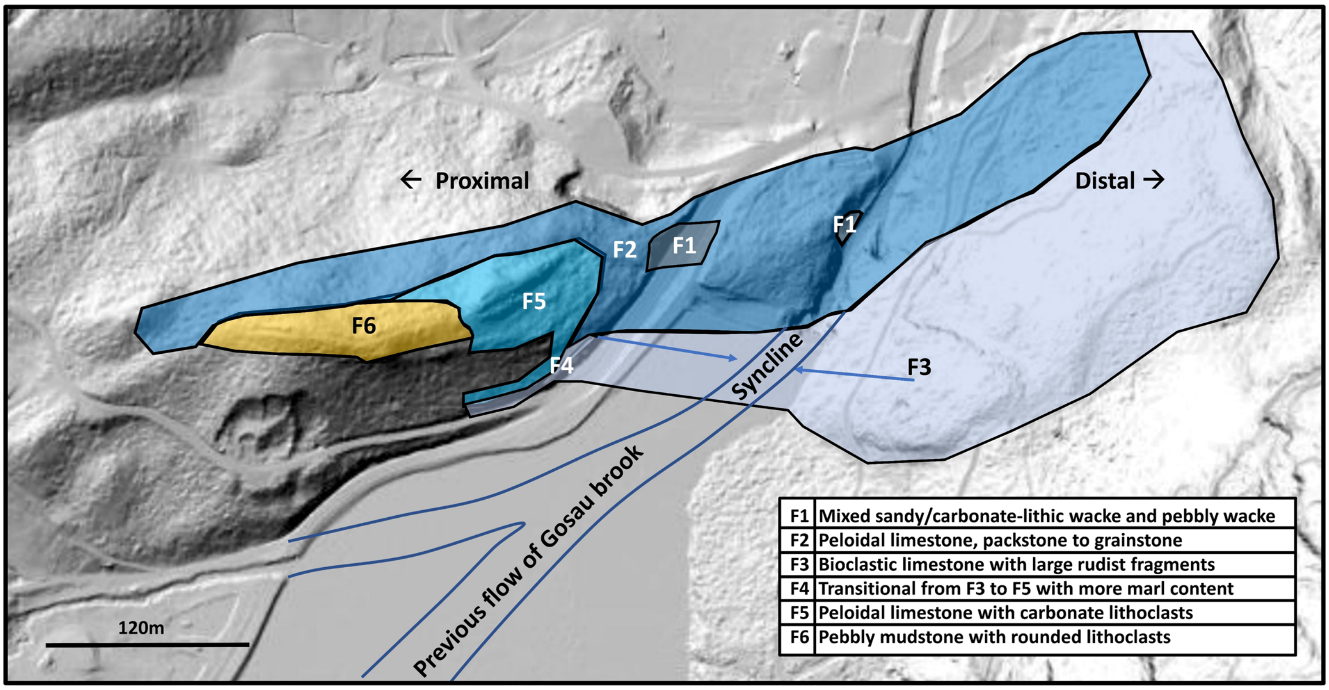

Figure 3: Map of the study area with the distribution of the six different facies types. The boundaries between the facies types are not sharp, but gradual, though there are a number of outcrops that appear to show the exact point of transition. From Digitales Oberösterreichisches Raum-Informations-System [DORIS], accessed on 24 January 2020.

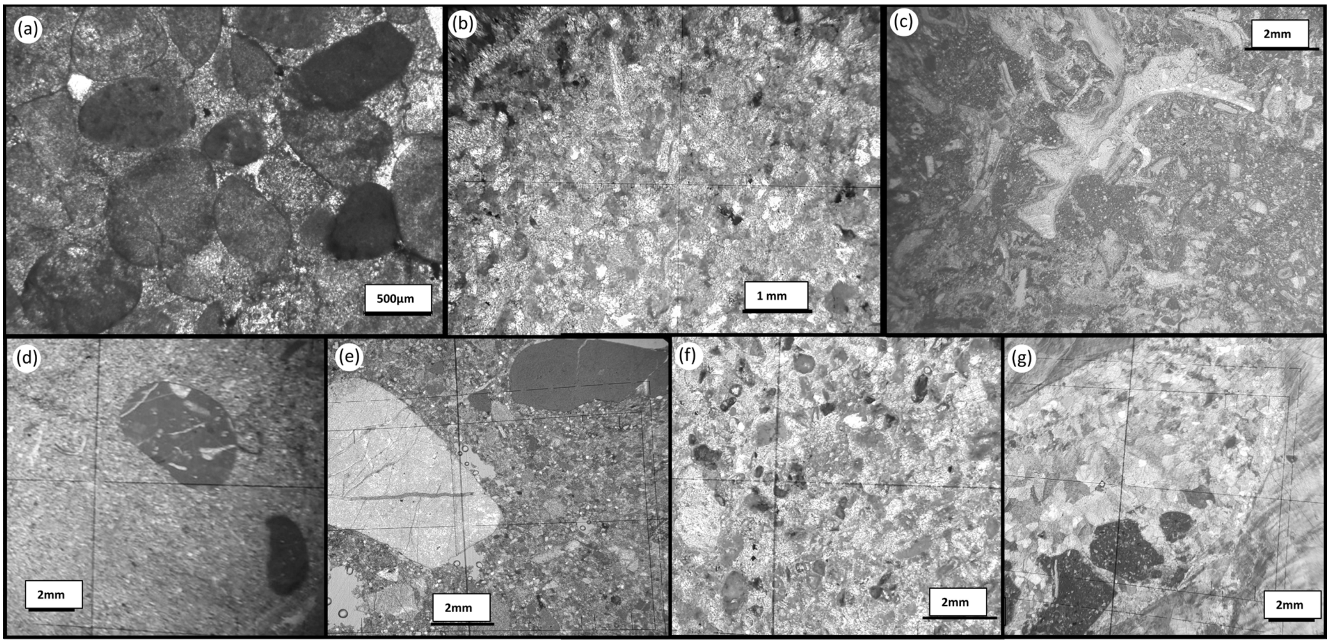

Figure 4: A: Facies Type F1, mixed sandy/carbonate-lithic wacke and pebbly wacke. **B**: Facies Type F2, peloidal limestone. **C:** Facies Type F3, bioclastic limestone. **D:** Facies Type F5, peloidal limestone with carbonate lithoclasts. **E**: Facies Type F6, pebbly mudstone with lithoclasts. **F**: Facies Type F4, transitional from F4 to F5, peloidal limestone with lithoclasts. **G**: Facies Type F4, bioclastic limestone with marl content, transitional from facies F3.

Type F6: Clast- to matrix-supported pebbly mudstone; small to very large rounded lithoclasts (Dachstein Limestone, quartz, chert) with a matrix of lime mudstone. Facies type F6 samples are brown to gray and the least competent lithology in the Hochmoos Formation at Gosauschmied. Fossil content is limited, while the peloidal components are very numerous.

Stratigraphically, the individual facies types transition from F1, the oldest, through F2, then F3 and F4, followed by F5 and finally F6, which comprises the youngest preserved sediments of the Hochmoos Formation in the study area.

Category	Characteristics	Subcategory	References, remarks
Arenite	Framework supported by sand grains; >50% siliciclastic sand and/or sand of carbonate rock fragments	Sandstone: >>50% siliciclastic grains Mixed siliciclastic/ carbonate-lithic arenite: roughly 50-50 Carbonate-lithic arenite: >>50% carbonate-lithic grains, without specification of mineralogy Calcarenite/doloarenite: mainly calcitic/dolomitic grains Hybrid arenite: mix of subequal amounts of bioclasts, carbonate-lithic grains and siliciclastic grains	Hybrid arenite/hybrid wacke: see, e.g., Zuffa (1985) for terms
Wacke	Sand grains supported by matrix	Sandy wacke: Mainly siliciclastic grains Mixed sandy/carbonate-lithic wacke Hybrid wacke: as above, but matrix-supported	
Pebbly arenite	Arenite with floating pebbles of silicic rocks and/or carbonate rocks; may also contain a few bioclasts	Subcategory with additional naming of pebble type: e.g., Pebbly arenite with carbonate lithoclasts	See Folk (1954, 1980) for more elaborate classifications of mixtures of pebbles, sand and/or mud
Pebbly wacke	Wacke with floating pebbles of silicic rocks and/or carbonate rocks; may also contain a few bioclasts	As above, but using 'wacke' instead of arenite	
Pebbly mudstone	Pebbles of silicic rocks and/or carbonate rocks floating in a typically marly matrix of silt- to clay-size grade (without or only with very few sand grains). Precise composition of matrix (relative percentage of clay minerals, carbonate mud and diverse silt-sized components) is not relevant	Subcategory with additional naming of pebble type: e.g., Pebbly mudstone with carbonate lithoclasts	
Biogenic limestones	More-or-less pure limestones that owe their origin to growth of organisms with calcareous hard parts, and to biological activity in general	Biogenic limestones are classified according to the modified Dunham (1962)–Embry and Klovan (1971) scheme (Wright, 1992)	

Table 1: Adapted terminology (see text) to characterize sediment textures and mixed carbonate-siliciclastic compositions.

Type	Description	Section in study area
F1	Mixed sandy/carbonate-lithic wacke and pebbly wacke	Core of anticline, beds 1–8 of profile W1, reflected on the east side of the Gosausee highway and along the brook
F2	Peloidal limestone, packstone to grainstone	Beds 9–24 of profile W1, area surrounding, base of profiles E1 and W2
F3	Bioclastic limestone with large rudist fragments	Profile E1 and surrounding area on east side of study area
F4	Transitional from F3 to F5 with more marl content	Profile W2 on west side of study area
F5	Peloidal limestone with carbonate lithoclasts	Immediately above profiles W1 and W2 in the forest to the west and up the ridge
F6	Pebbly mudstone with rounded lithoclasts	Above facies F5 and terminating at the top of the ridge on the west side of the study area

Table 2: Overview of the six different facies types of the Hochmoos Formation in the study area at Gosauschmied.

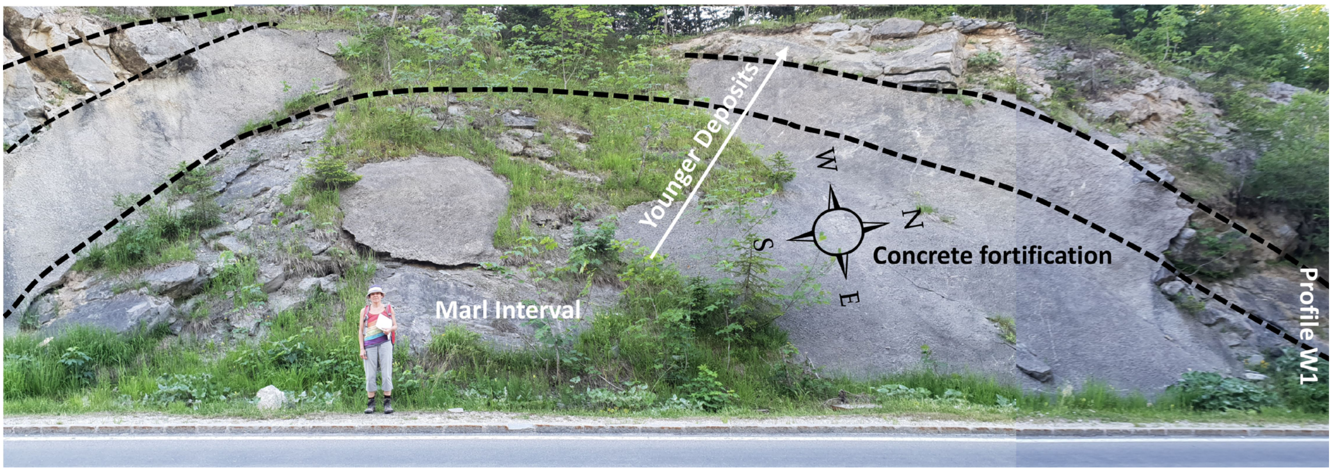

Figure 5: Composite photo of the anticline core in the study area with bedding indicated by the dashed lines. The beginning of profile W1 can be seen at the north end of the anticline. The marl interval at the center indicates the oldest deposits, with an arrow showing the direction of younging.

4.2 Stratigraphic analysis

4.2.1 Base of section

The Gosauschmied anticline exposed in the base of the section is one of the most significant geological structures in the study area. The anticline forms a morphological ridge extending from west to east, thus dividing the western part of the study area: outcrops on the northern limb dip to the N/NE, while outcrops on the southern limb dip to the S/SE (strike/dip symbols in Fig. 2). The fold axis is reconstructed to dip to the east at approximately 14° (reconstruction in Kearney, 2020).

Together with other outcrops on the west side of the study area, the anticline was exposed in the course of road works for the Gosausee highway. A concrete fortification structure was required to shore up this area to prevent rock slides onto the road; hence a large portion of the anticline is covered. The anticline includes the base of profile W1 (Fig. 5), which constitutes the north end of the anticline. The core of the anticline contains the oldest sediments in the study area, consisting of marls, gradually transitioning to mixed sandy/carbonate-lithic wacke and pebbly wacke with carbonate lithoclasts (F1), as evidenced in the first 7 beds of profile W1. These are overlain by peloidal limestone (F2), which can be found in both limbs of the anticline and extending into the forest.

The marls in the core of the anticline show small calcareous tests and shell fragments on their weathering surfaces. Sieved fractions from the marls mainly contain terrigenous components (grains of clay and calcite), in addition to calcareous tests and shell fragments. Most of these were fractured and overgrown and hence could not be identified. Several intact microfossils, such as ostracods and miliolid foraminifera, were also found.

4.2.2 Profile W1

Profile W1 is located on the west side of the Gosausee highway. It consists of a lower package of mixed sandy/carbonate-lithic wacke and pebbly wacke with carbonate lithoclasts (F1), followed by a thin marl layer (F1) and, above, a package of thick medium- to dark-gray peloidal limestone beds (F2) (Fig. 6, stratigraphic column in Fig. 7). The dip angle is variable and ranges from 33° to 62° in a N/NE direction, tending toward true N in the highest (youngest) beds of the profile. Fossil content is low and, in some beds, non-existent. Figure 6 shows the first part of profile W1 up to the marl layer at bed 8. These beds are part of the core of the anticline and are mirrored on the south side of the anticline (Fig. 5).

Profile W1 consists of 24 beds and has a thickness of a bit more than 17 m. The outcrop is no longer exposed at its most NE point. Bed 1 of profile W1 was selected as the first exposed portion of the outcrop north of the concrete fortification structures covering the anticline (Fig. 6).

Microfacies – Profile W1

The thin sections created from the first 7 beds show some fossil content, but this is primarily restricted to singular benthic foraminifera. From bed 1 through bed 5, the terrigenous clasts are medium to coarse-grained and consist of sand, quartz, chert and carbonate lithoclasts from Dachstein Limestone, often containing Triassic fossils, such as involutinida and biserial agglutinating (textularida) foraminifera. Bed 4 is highly dolomitized. Beds 7–13 in profile W1 represent a transition from a pebbly wacke with carbonate lithoclasts (F1) to a much purer limestone with only limited terrigenous content (F2). Bed 8 consists of a thin marl layer. Samples taken from this bed contained only a few nannofossils, but these clearly indicated a fully marine deposition. Beds 9–13 (F2) gradually transition into dark-gray to medium-gray peloidal limestone with, initially, some marl content that totally disappears by bed 14. Fossil fragments appear to be allochthonous based on their broken character, and there are only small and scant instances of Dachstein Limestone. As of bed 14, profile W1 transitions into a rather monotone succession of medium-gray peloidal limestone beds (F2) with almost no terrigenous/

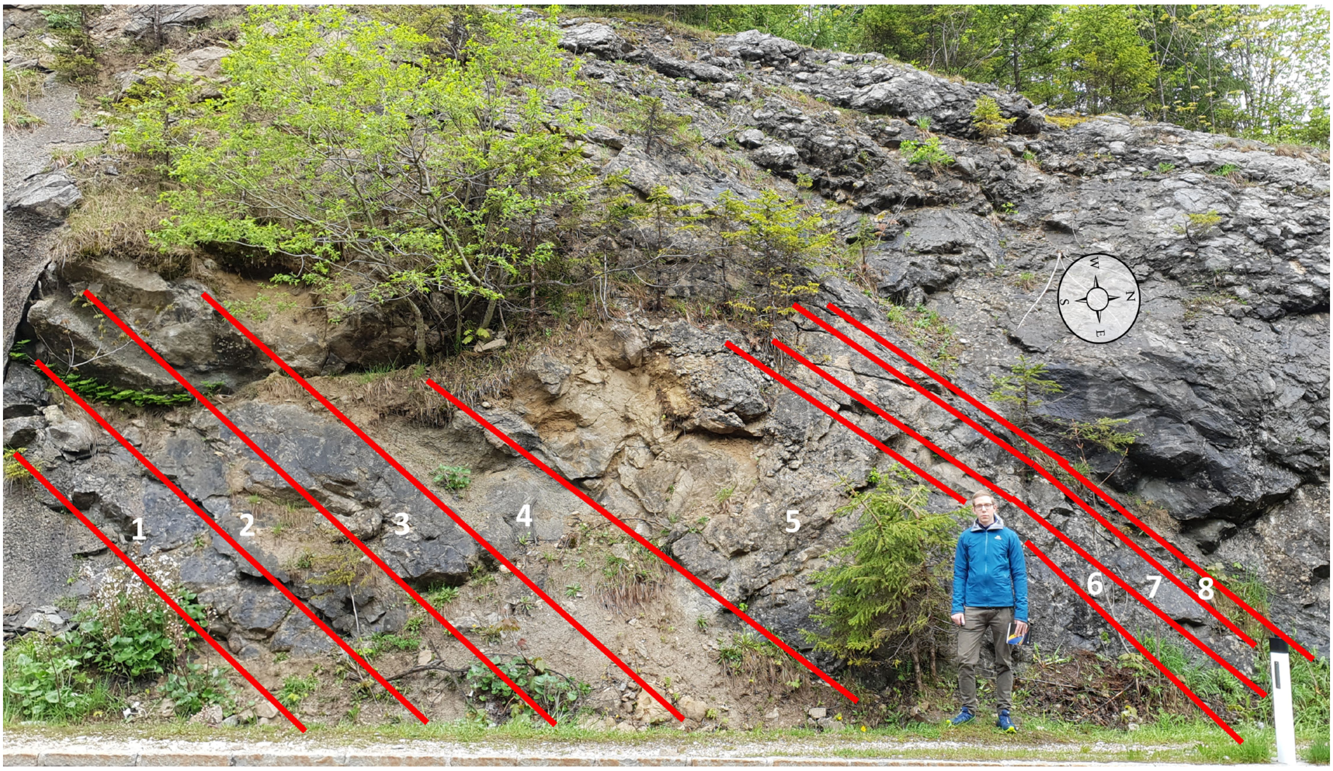

Figure 6: View of profile W1: the first eight beds are indicated by the red lines.

siliciclastic components and very low fossil content: apart from a few scattered foraminifera and biogenic fragments, there is little to distinguish the different beds from each other. The final bed in the profile, #24, is the least differentiated.

Outcrop south of Profile W1 and core of anticline

This part of the outcrop along the Gosausee highway correlates to profile W1 and constitutes the southern limb of the anticline, which extends above W1 and is stratigraphically below W2. However, due to brittle faulting and the strongly-deformed nature of the outcrop, no section could be adequately logged. Thin sections from samples extracted from this outcrop show the same trends as in Profile W1, with lithologies ranging from pebbly wacke with carbonate lithoclasts (F1) to peloidal limestones (F2) with very scant fossil content (mainly benthic foraminifera and solitary rudist fragments of allochthonous origin).

4.2.3 Profile W2

Profile W2 is located south of the anticline and overlies equivalents of profile W1. It is made up of six beds of varying thickness and totals up to 6.5 m (Fig. 8). Profile W2 consists of very thick, nearly horizontally-positioned dark marly limestone beds (F4). The dip direction is S/SE at moderate angles (25–48°) (Fig. 9, legend Fig. 7).

The sediments of profile W2 continue into the woods to the west of the road and the outcrop. The lithology of profile W2 is compact and tends toward bioclastic wackestone and packstone and only rarely rudstone and floatstone (beds 1 and 2). The larger biogenic components gradually disappear from the older to the younger beds in the outcrop. The youngest bed (6) has more features in common with outcrops found in the woods above profile W2 than with beds 1 and 2 at the base.

The first two beds in profile W2 consist of dark, marly limestone that is much more brittle than the peloidal limestone of profile W1. These have the greatest fossil abundance in the outcrop: radiolitid macrofossils were identified in the face of bed 1 and weathering out of both beds 1 and 2. The thin sections were likewise rich in fossil specimens and had much in common with the bioclastic limestone with large rudist fragments found in profile E1 (F3), though the samples from which they were created were much darker on the surface due to marl content. The remainder of the beds in profile W2 also have fossil content, but in a diminishing fashion as the sediments get younger. Regarding macrofossils, large *Durania* sp. specimens were identified in beds 1 and 2. One fragment was extricated and used for Sr-dating (for images of these macrofossils, see Kearney, 2020).

Microfacies analysis – Profile W2

Profile W2 (F4) represents a gradual transition from bioclastic limestone with rich fossil abundance at the base (beds 1 and 2) to a hybrid bioclastic/peloidal limestone at the top (bed 6). There are fossils throughout the outcrop; but they become smaller and less numerous in the higher (younger) strata of profile W2. At the same time, peloids

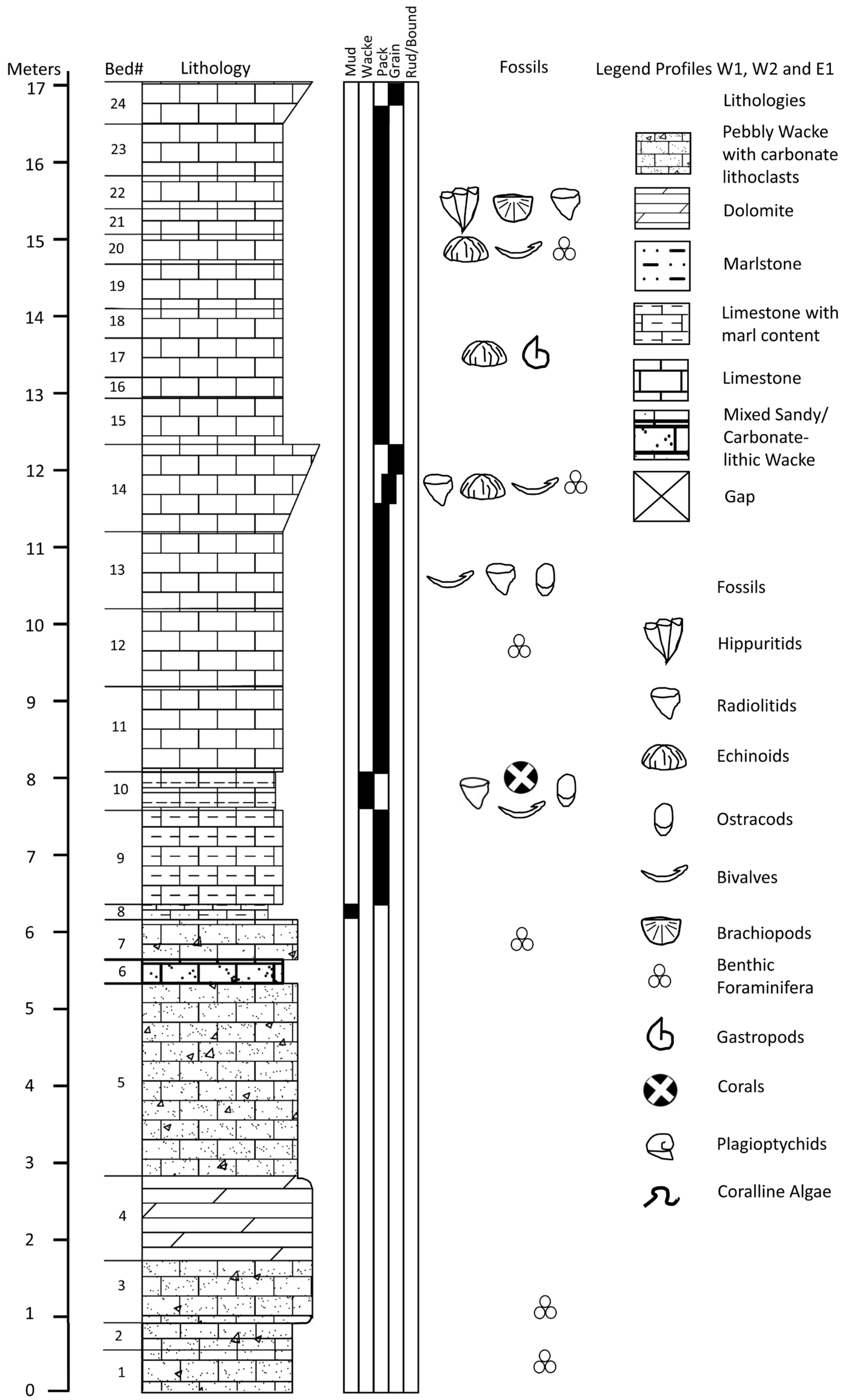

Figure 7: Stratigraphic column of profile W1, Hochmoos Formation, Gosauschmied (N 47.550141, E 13.514879, 780 m).

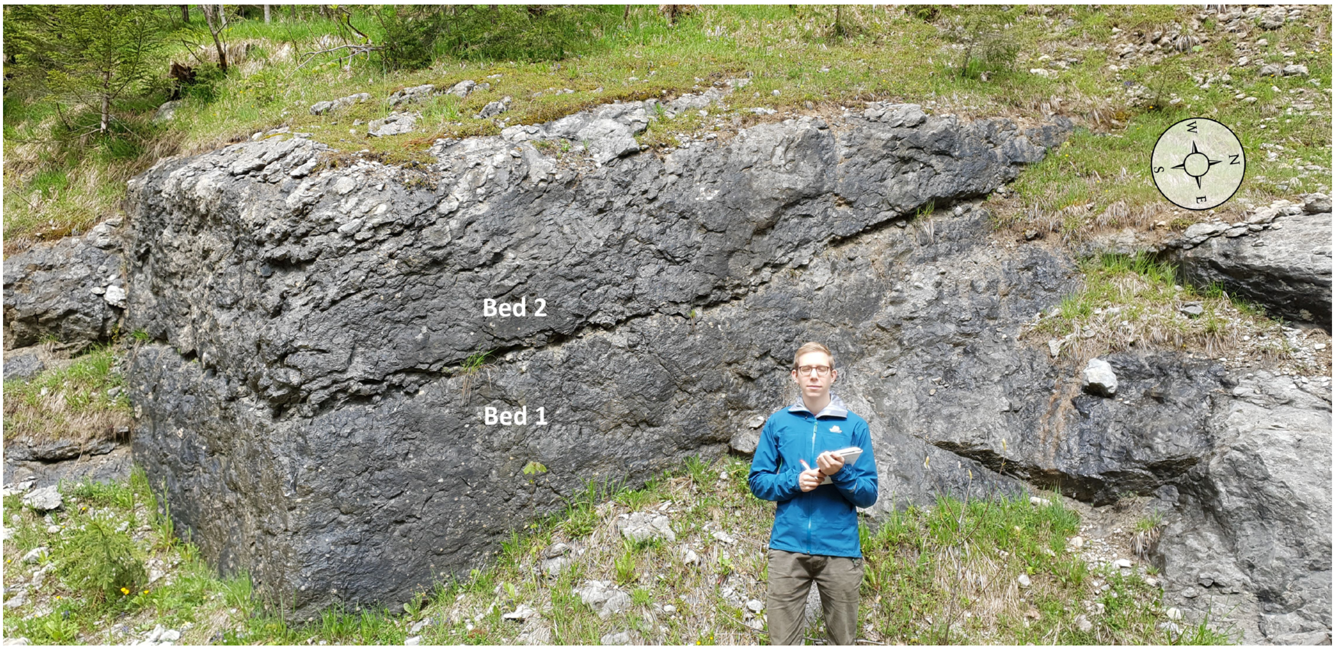

Figure 8: Photo of profile W2 along the Gosausee highway, with beds 1 and 2 indicated.

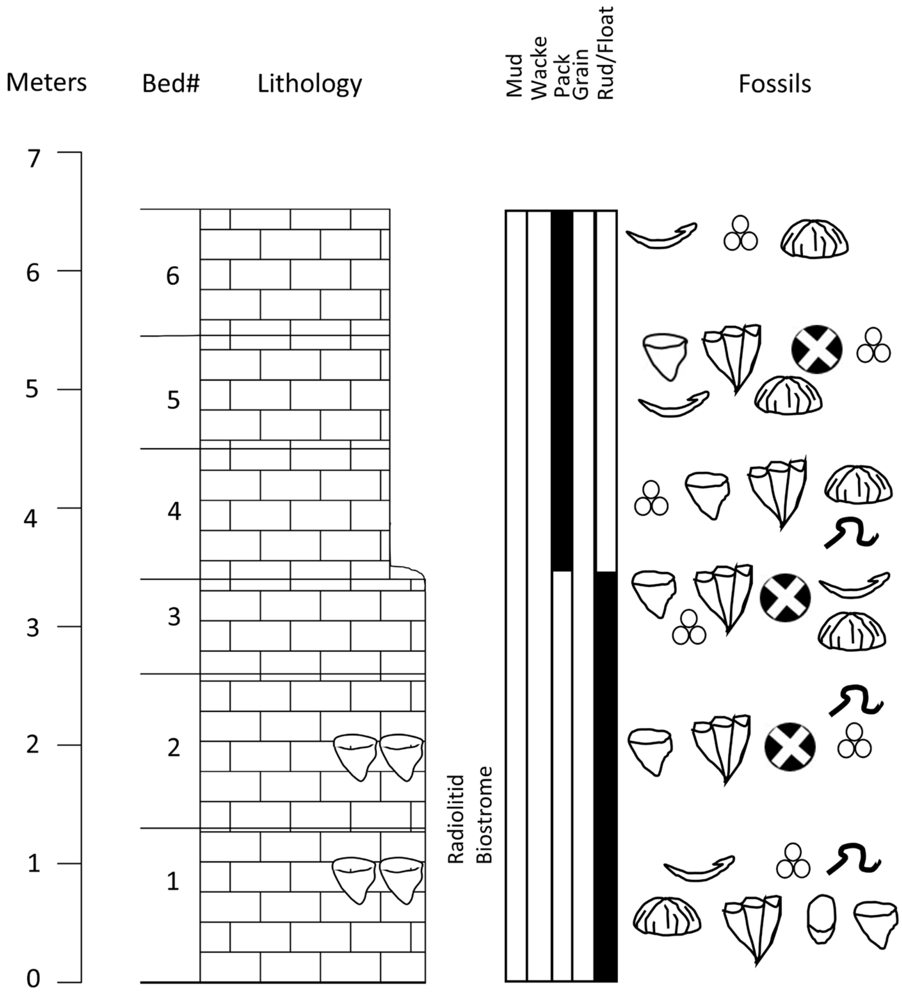

Figure 9: Stratigraphic column of profile W2, Hochmoos Formation, Gosauschmied (N 47.549332, E 13.513960). Legend in Figure 5.

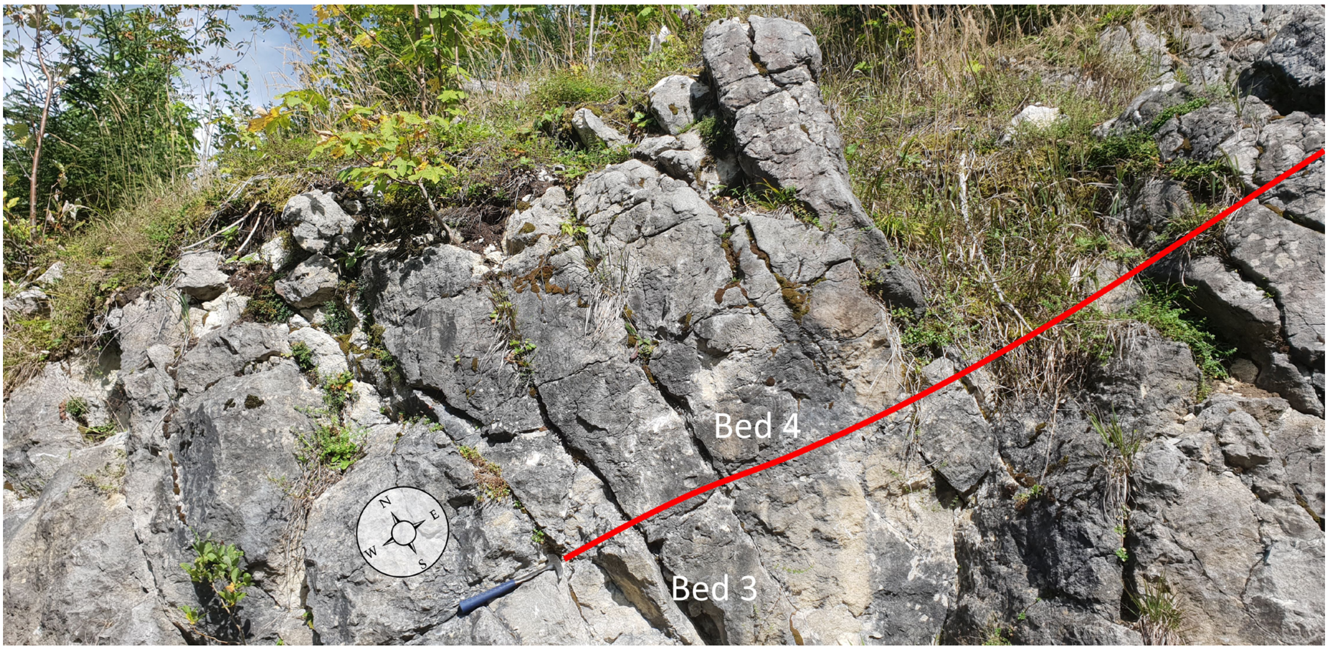

Figure 10: Profile E1 near the Geotrail. The picture shows the orientation of joints running orthogonally to the actual bedding orientation (red line, beds dip at 30° – 45° in the direction of W/NW).

and other clastic components become more abundant. The thin sections from the first beds of profile W2 have more in common with profile E1 than profile W1. By bed 6, this situation is reversed. Profile W2 and the sections immediately above are also the only outcrops in the study area that evidence coralline red algae in the thin sections. These are not found in W1 or E1.

4.2.4 Section parts above profiles W1 and W2

There are numerous outcrops above profiles W1 and W2 in the forest and up the ridge to the top of the Hochmoos Formation, extending as far as the boundary with the Bibereck Formation. In total, 32 separate outcrops were investigated in the forest area above profiles W1 and W2 (Kearney, 2020).

The morphology of the hill and ridge behind profile W2 and the orientation of the beds in profile W2 indicate that the strata in profile W2 continue at higher elevations. One clear difference, however, was the lighter color (medium gray, lower marl/clay content, more peloidal content). Also, the Dachstein Limestone clasts in the thin sections were larger, indicating more terrigenous input. Similar to bed 6 in profile W2, there was fossil content, but limited to individual foraminifera and fragments (corals, echinoid, inoceramid). Fossil content continued to decrease in the younger (higher) strata.

A very marked change (F5) occurred at an outcrop along the ridge (795 m a.s.l., N: 47.550039, E: 13.514152): samples taken here showed visible evidence of carbonate lithoclasts (0.5–1 cm dia.), which could be noted in at least two other outcrops in the vicinity. By contrast, there were three outcrops further up the ridge that had no visible carbonate lithoclasts on a macro level and reverted back to a peloidal limestone lithology of packstone to grainstone.

Further up the ridge at an elevation of around 825 m a.s.l., first evidence of a pebbly mudstone with a clayey-silty matrix appeared (F6), replacing the peloidal limestone lithology (F5); and the clasts (carbonate lithoclasts, chert, quartz) increased in size (1–3 cm dia.) up to the very top of the ridge at 831 m a.s.l. At the next outcrop down the incline and slightly to the east (824 m a.s.l., N: 47.549662, E: 13.512372), there is a bed that appears to contain the actual facies boundary between the peloidal limestone with carbonate lithoclasts and the overlying pebbly mudstone.

Roughly 75 m from the forest road at 820 m elevation (a.s.l.), the pebbly mudstone with rounded lithoclasts (F6) reverts back to peloidal limestone with no visible clasts (F5). Directly next to the forest road at 817 m a.s.l., the outcrop there again looked very much like the pure peloidal limestone beds in the younger beds (14–24) of profile W1 (F2).

4.2.5 Profile E1

In the eastern part of the study area, Profile E1 was selected for a thorough and detailed survey (Fig. 2). This outcrop is the most extensive in the study area with a lateral exposure of 31 m and, owing to its fossil richness, constitutes one stop on the Gosau Geotrail.

Profile E1 consists of 10 extensive beds of light-gray bioclastic limestone with large rudist fragments, totalling a thickness of 15.4 m (stratigraphic column in Fig. 11) and running from the Geotrail at 798 m a.s.l. up to about 815 m a.s.l. at the top. The sediments continue past the top of bed 10, but increasing gaps in the stratigraphic

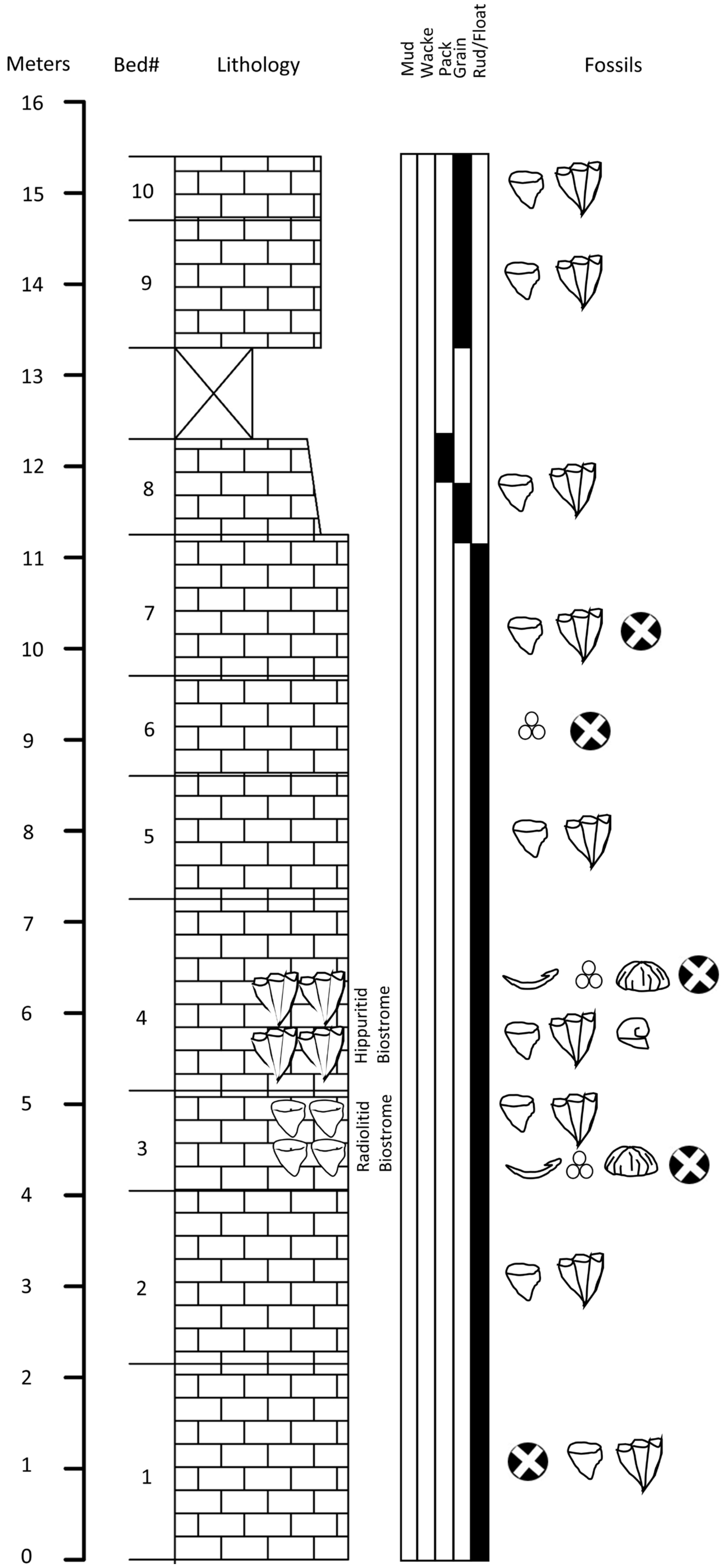

Figure 11: Stratigraphic column of profile E1, Hochmoos Formation, Gosauschmied. (N 47.549107, E 13.516171). Legend in Figure 5.

succession hamper correlation of beds. However, this whole section was sampled for carbon and oxygen isotope analysis. Profile E1 shows joints (E/SE at 60°) orthogonal to the actual bedding direction (W/NW at 30°), which is indicated by the orientation of fossils in the outcrop (Fig. 10).

Fossils are abundant throughout profile E1. Macrofossils are visible as specimens weathering out of the rock or as markings on the face of the rock. There are also a number of rudist biostromes at various positions in the outcrop in beds 3 and 4. There is a uniformity to the facies (F3) of profile E1: the samples show a much lighter color than profile W1, and this is due primarily to the presence of rudist fragments, micrite cement and significant sparite infillings in the hollow chambers of fossil organisms. The only exception to the otherwise uniform facies consists of the isolated occurrences of radiolitid and hippuritid biostromes in beds 3 and 4.

Microfacies and biofacies analysis – Profile E1

The variety of fossils is limited and primarily dominated by radiolitid and hippuritid shell detritus. Plagioptychids appear, but only sporadically. Corals are frequently found in the fabric cohabiting with the rudists, often encrusting upon them. Foraminifera occur in isolated instances (Miliolina, Textularina), as do echinoids (primarily remains of sea urchins). The non-biogenic components consist of some peloids, but the vast majority of the matrix is composed of micrite, while sparite and a bioclastic dark brown sediment with marl content are commonly found in the hollow chambers of biogenic components. The hippuritid and radiolitid shells, in some instances, have been thoroughly or partially micritized, or fully replaced with sparite. In a few cases, sediment infillings were encased by sparite or micrite left over from shells that had been fully diagenetically leached. In many cases, however, the original shell was intact with its primary calcite make-up. The outcrop (F3) can be subdivided into three sections: 1) beds 1–2 consist mainly of bioclastic limestone with large rudist fragments, 2) beds 3–4, which are the most extensive and, in some places, indistinguishable from each other; these two beds consist of bioclastic limestone with large rudist fragments and contain the only biostromes identified in the outcrop, 3) beds 5–10 have no exposed biostromes, but possess a lithology (floatstone to rudstone) and fossil content very similar to beds 1 and 2 at the base of the outcrop and beds 3 and 4 between the biostromes.

In bed 3 of profile E1, numerous radiolitid fossils were identified and proved to be a radiolitid biostrome: these are, in contrast to hippuritid biostromes, less orderly in their growth patterns, with the colony having a more heterogeneous structure. This particular sample also evidenced sparse hippuritid cohabitation. At the base of bed 4 in profile E1, a very large fossil sample of a portion of a hippuritid biostrome was found. A cut of this sample just beneath the upper valve of the rudists in the biostrome, together with cross-sections identified in the thin sections, showed this particular organism to be *Vaccinites* sp., with the species indeterminate (potentially *V. sulcatus* or *alpinus*). Near the base of bed 4 in profile E1, a large radiolitid fossil was identified, though to date no genus could be assigned to it. Its identification as a radiolitid could be determined due to the so-called celluloprismatic mesostructure (Skelton, 2013) typical of the family Radiolitidae and evident in the thin sections of radiolitid rudists (for more details and images, see Kearney, 2020).

4.2.6 Area surrounding Profile E1

Profile E1 and Surrounding Plateau

Profile E1 represents the southern margin of a topographic plateau (1800 m^2) composed of bioclastic limestone with large rudist fragments. Dip direction was NW at angles between 20–40°. Along the west side of this plateau, a sequence of large (2 m high) light-gray limestone outcrops with no apparent bedding consists of grainstone with a smooth, hard surface and no macrofossils. These massive outcrops are interspersed with smaller, less prominent beds of bioclastic rudist limestone with macrofossils. Near the top of the plateau to the east, the outcrops resemble the lithologies of profile E1. At the north margin of the plateau, prominent outcrops (4 m and higher) of bioclastic limestone with large rudist fragments evidence lithology and macrofossil content also very similar to profile E1 (F3). Samples were taken from outcrops along this plateau for use in the carbon and oxygen isotope measurements.

Area north of Profile E1 and the plateau

A total of 12 outcrops were investigated to the immediate north of E1 (Kearney, 2020). The lithology of these outcrops was very similar and showed a clear continuation of the medium- to light-gray bioclastic limestone of profile E1 and its immediate surroundings. Macrofossils could be seen in all but two outcrops. The dip direction was N/NW at 30-40°.

The area to the north of profile E1 is lithologically, structurally and stratigraphically connected to profile E1. The very few outcrops identified between the Geotrail and the reservoir showed a further continuation of this macrofossil-bearing bioclastic limestone facies.

4.2.7 Gosau brook and hydroelectric power station

The west and east parts of the study area are divided by the Gosau brook and the reservoir behind the hydroelectric power station. The front edge of the dam is at an elevation of 780 m a.s.l. Roughly 50 m downstream from the base of the dam, the outcrops and the bedding are regular and provided consistent structural measurements, which were aligned with the N/NE dip direction of profile W1 north of the anticline. However, the outcrops near the dam (between 0 – 50 m) on the west side of the brook provided no consistent structural measurements due to faulting in the area. On the east side of the dam, measurements at the top above the brook and near the base of the dam showed the W/NW dip direction of profile E1.

With respect to lithology, all the samples were peloidal limestone with packstone to grainstone texture, with a higher percentage of grainstone on the west side of the brook than on the east side. The character of the limestone was very similar to the samples at profile W1 (peloidal limestone), though the general color was lighter and grew lighter from the west side to the east side. None of the samples in the immediate vicinity of the brook contained macrofossils. Immediately above this area on the east side, however, (i.e., from the Geotrail down to the top of the dam) macrofossils typical of profile E1 continued, then disappeared at a point roughly five meters from the top of the dam. This is a clear facies boundary between the bioclastic limestone with rudist fragments (F3) characteristic of profile E1 and the peloidal limestone (F2) characteristic of profile W1 and the area around the Gosau brook. At the west side of the brook (>50 m from the dam to the north), beds comprising the last exposed portion of the core of the anticline (pebbly/sandy wacke, F1) could be identified, as well as peloidal limestone (F2) outcrops with dip direction aligned to profile W1 (N/NE). No corresponding outcrops on the east side of the brook could be identified.

4.3 Strontium, carbon and oxygen isotopes

4.3.1 Strontium isotope ratios

Five separate measurements of strontium ratios ($^{87}Sr/^{86}Sr$) were taken (Tab. 3), including three samples (B1, B41, B44) from profile E1 using rudist shell material (bed 4), one sample (C1) from profile W2 using the *Durania* sp. specimen from bed 1 and one sample (CW11) from an outcrop along the ridge above profile W2 using a limestone sample.

Wolfgring et al. (2018) at the Gosau locality of Postalm used a combination of strontium isotope measurements, index fossils and paleomagnetic data to establish a reliable $^{87}Sr/^{86}Sr$ ratio of 0.707534 (mean of 4 analyses) at the paleomagnetically-defined Santonian/Campanian boundary. For this period, values greater than this represent a younger (Campanian) age, while values lower than this are of Santonian (or older) age.

The mean value taken from Wolfgring et al. (2018) at the Postalm is included as a reference for the Santonian/Campanian boundary applicable to Upper Cretaceous marine carbonate sediments of northwestern Tethys origin.

4.3.2 Carbon and oxygen isotopes

Figure 14 shows the plots of the $\delta^{13}C$ and $\delta^{18}O$ isotope values for profile W1 and profile E1 as a composite. In the case of profile W1, the samples were extracted from the last 10.9 m of the outcrop, which contain the marl layer and the pure limestone beds. Mean sample resolution was 64cm. The samples from profile E1 included 10 from the outcrop itself and another 8 taken from outcrops that could be correlated to E1 and extended up the ridge to the boundary of the Hochmoos Formation with the Quaternary sediments (Fig. 2). Mean sample resolution for these measurements was 500 cm. Values were also obtained for profile W2, but the sample number (6) and resolution (110 cm) did not produce a meaningful individual curve. Stratigraphically, W2 correlates to the lower beds of profile E1.

Sample	$^{87}Sr/^{86}Sr$	+/-2sm	Latitude	Longitude
C1	0.707515	0.000004	47.549332	13.513960
CW11	0.707549	0.000004	47.549807	13.513452
B1	0.707485	0.000004	47.549107	13.516171
B41	0.707508	0.000008	47.548980	13.516506
B44	0.707514	0.000007	47.548973	13.516511
Wolfgring 2018	0.707534	mean value	47.610500	13.385417

Table 3: Strontium isotope measurements from Gosauschmied compared to the mean value for the base of the Campanian at the Postalm from Wolfgring et al. (2018).

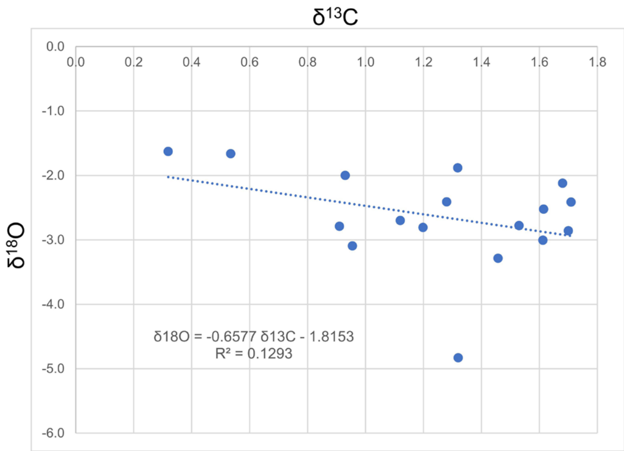

Figure 12: $\delta^{13}C$ (x) plotted vs. $\delta^{18}O$ (y) values for profile W1. Best fit line and correlation (R^2) for the plot is included.

5. Discussion and Interpretation

5.1 Chronostratigraphy

Four of the five ratios derived from samples in Gosauschmied (3 in profile E1 and 1 in profile W2) are lower than the reference ratio at the Santonian/Campanian boundary at the Postalm and are hence in the late Santonian. Furthermore, two of the values from profile E1 and the one from the lower part of profile W2 show similar values (0.707508 B41, 0.707514 B44 and 0.707515 C1), indicating roughly synchronous deposition. The $^{87}Sr/^{86}Sr$ ratio from the sample taken along the ridge behind profile W2 (see Tab. 3) is 0.707549 and thus, assuming no diagenetic contamination of the sample, in the Campanian. This is stratigraphically the highest sample taken for Sr isotope stratigraphy, and therefore a younger age compared to all others at Gosauschmied is in accordance with this stratigraphic position on top of the anticline ridge. Moreover, according to Trenkwalder (1999, p.133), the LGS occurrences at the SE margin of the Gosau basin, particularly the Hochmoos Formation, have a higher relative stratigraphic position (partially due to reduced thickness) than comparable occurrences at the basin center; and this appears to cause a relative descent of the Santonian-Campanian boundary along a NW-SE gradient compared to the uppermost Santonian lithostratigraphic boundary of the Hochmoos Formation in the basin center (e.g., Wagreich et al., 2010), potentially resulting in an earliest Campanian age for the youngest sediments in the Hochmoos Formation in localities such as Gosauschmied and others (Schmiedsippl, Katzhofgraben) at the SE basin margin.

The $^{87}Sr/^{86}Sr$ measurements taken in key areas of the Hochmoos Formation at Gosauschmied thus confirm a late Santonian age and provide a strong chronological correlation between the two separate parts of the area (west and east). A sample from the basal Bibereck Formation (N:47.551289, E:13.509667) in Gosauschmied showed the typical assemblage of the late Santonian to earliest Campanian nannofossil zone CC17b, including *Calculites obscurus* and curved *Lucianorhabdus cayeuxii* without *Broinsonia parca parca*, thus denoting the Santonian-Campanian transition, as already known from the upper Santonian at the nearby sections of Schattau (Wagreich et al., 2010) and Postalm (Wolfgring et al., 2018).

The results from the $\delta^{13}C$ and $\delta^{18}O$ measurements provide a lower degree of chronostratigraphic certainty, primarily due to the missing section continuity and the low resolution of samples taken from isolated profiles W1, E1 and W2. With a mean sample resolution of 64 cm for profile W1 and only 17 measurements covering 10.9 m, the resulting curve on its own cannot be reliably correlated with any standard (e.g., Jarvis et al., 2006). With respect to profile E1, the 36 m range in the outcrop is more significant, but the sample resolution (avg. 500 cm due to missing section continuity) is quite low for such an extensive profile. What remains quantitatively unresolved is the magnitude of the gap between the two profiles (ca. 1–10 m based upon relative elevation and structural data). W2 correlates biostratigraphically and isotopically to beds 3–6 in profile E1 and hence is not included in this discussion. Nonetheless, the $\delta^{13}C$ curve resulting from the 18 samples for profile E1 implies a negative peak at the beginning followed by a double positive peak probably correlating to the Santonian/Campanian boundary event (SCBE) (Wolfgring et al., 2018; Jarvis et al., 2002, 2006; Thibault et al., 2016). However, the position of the Santonian/Campanian boundary in relation to first and last appearances of planktonic markers and the carbon and strontium isotope stratigraphies is not confirmed, as a GSSP definition of the base of the Campanian has not yet been established (see discussion in Wolfgring et al., 2018). The plot of the $\delta^{18}O$ vs. the $\delta^{13}C$ values for both profile W1 (Fig. 12) and profile E1 (Fig. 13) shows no statistically significant correlation, hence there does not appear to be significant diagenetic impact on the results.

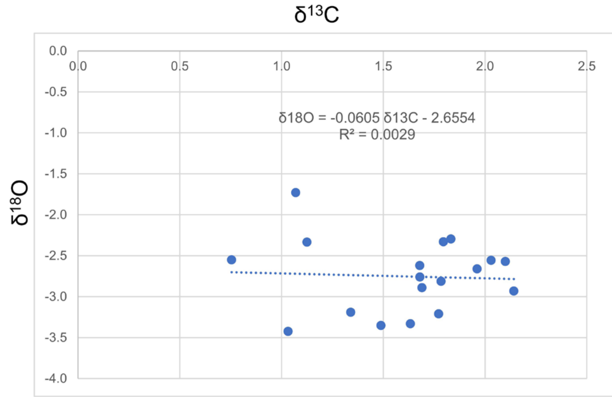

Figure 13: $\delta^{13}C$ (x) plotted vs. $\delta^{18}O$ (y) values for profile E1. Best fit line and correlation (R^2) for the plot is included.

Using the composite $\delta^{13}C$ curve of profile W1 and E1 (Fig. 14), a number of key excursion events can be identified and, with some caution, correlated to the reference curve in Jarvis et al. (2006). These events (Buckle, Hawk's Brow, Foreness and the SCBE) represent prominent positive and negative excursions from the upper Santonian to the boundary with the Campanian (Jarvis et al., 2006; Wolfgring et al., 2018). This provides further support for a latest Santonian age for the greater part of the Hochmoos Formation in Gosauschmied. Furthermore, when correlating this excursion data to absolute timespans as documented in Thibault et al. (2016), an approximate sedimentation rate can be calculated. The total sampled extent of profiles W1 + E1 results in a thickness of at least 47 m (neglecting the unsampled basal part of profile W1 and the stratigraphic gap between W1 and E1; see Tab. 4). Data from Thibault et al. (2016) indicate that the $\delta^{13}C$ excursion events recorded in the composite curve for profiles W1 and E1 span 800 to 1200 ka, with a mean of 1000 ka. This results in an estimated sedimentation rate of 47 mm/ka, which is significantly more than pelagic sedimentation rates (19.9 mm/ka) calculated at Postalm by Wagreich et al. (2012), but modest for shallow marine carbonate settings in the Late Cretaceous (as high as 100 mm/ka; e.g., Pohl et al., 2020).

An estimate for marine water temperatures based on the $\delta^{18}O$ values between -2 and -4‰ indicates paleotemperatures of 20 to 29°C (conservative estimates for an ice-free world using equations of Anderson and Arthur, 1983; see also Zakharov et al., 2017).

Summing up, in the absence of diagnostic biostratigraphic macrofossil data, a late Santonian age is confirmed for the greater part of the studied Hochmoos Formation rocks in Gosauschmied based on the following reasoning: (1) The benthic foraminifer *Nummofallotia cretacea* is present in several of the carbonates and rudist-bearing beds, and was determined to be typical for the upper Santonian of the Schattau section of the Hochmoos Formation (Wagreich et al., 2010); (2) scarce

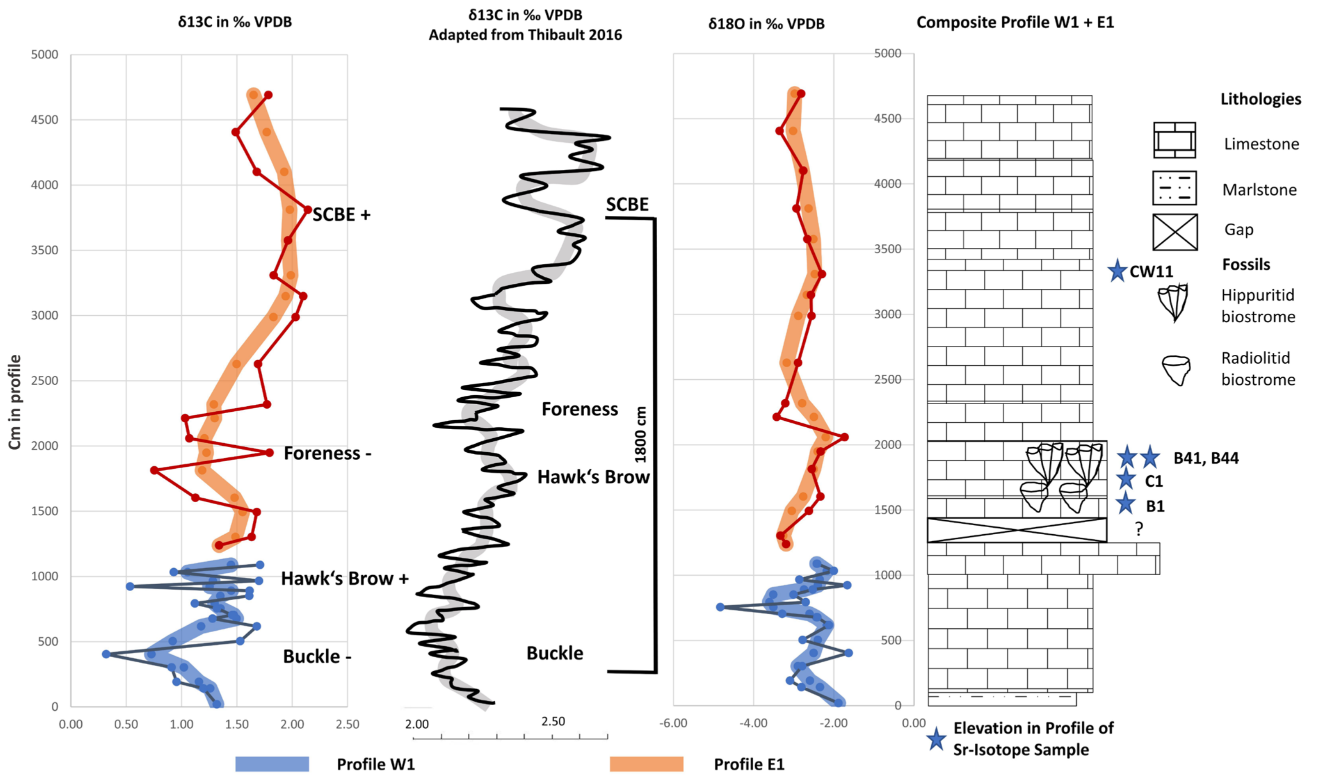

Figure 14: Composite $\delta^{13}C$ and $\delta^{18}O$ curves for profiles W1 and E1 using a three-point rolling average (broad curves). The original data points are included as a thin line plot. Key $\delta^{13}C$ excursion events from Jarvis et al. (2006) are correlated to the data, with a reference curve adapted from Thibault (Seaford Head, Fig. 2, 2016), with the broad light gray curve representing a three-point rolling average and the individual data points shown on the thin black curve. Lithologic succession of profiles W1 and E1 is included for reference, with the height in the profile of the Sr-Isotope samples indicated (see Tab. 3).

calcareous nannofossil data at Gosauschmied indicate the late Santonian to earliest Campanian CC17b of Wagreich (1992) up to the base of the Bibereck Formation; (3) Strontium isotope stratigraphy shows a late Santonian age for 4 of the 5 samples, with only the uppermost sample showing a value in the Campanian age range, which accordingly may indicate that the Santonian/Campanian boundary is located within the upper part of the Gosauschmied carbonate succession; (4) carbon isotope values show a negative peak at the base of profile E1, followed by a positive broad double peak, which may correlate to the SCBE and hence infer an even lower position of the Santonian/Campanian boundary within the extension of profile E1 on the east side of the study area. Thus, the lower part of the studied succession is of (late) late Santonian age; the base of the Campanian (as defined by a correlation to the magnetostratigraphy data by Wolfgring et al., 2018) may be within the extension of profiles E1 or W2 in the uppermost Hochmoos Formation.

5.2 Deposition Scenarios and Sequence Stratigraphy

5.2.1 General considerations

The sediments of the Hochmoos Formation in the Gosau basin represent coastal and shallow-marine deposits and structures, including small reefs that primarily consisted of rudists, corals and combinations of these. According to Sanders and Pons (1999), varying depositional settings are responsible for the wide range of facies found in the LGS, particularly with respect to the development of rudist colonies. Sanders and Pons (1999) distinguish between three types of siliciclastic-dominated cycles and three types of carbonate-dominated cycles. Specifically, the type B carbonate-dominated cycle in their work is ascribed to rudist formations found in the LGS of the Gosau basin, which are mainly stratigraphically positioned in the Hochmoos Formation such as the Brunftloch at Wegscheidgraben near the Pass-Gschütt (Kollmann and Summesberger, 1982; Höfling, 1985; Wagreich, 1988). This outcrop has a thickness of roughly 11 m, contains two rudist biostromes and is stratigraphically positioned in the upper Hochmoos Formation (Wagreich, 1988). However, in contrast to the lithology found in Gosauschmied, the outcrop at Brunftloch contains a much higher quantity of sediments composed of arenites and wacke (both pebbly and sandy), indicating a depositional setting with more terrigenous/siliciclastic input. A further notable example of a rudist-dominated outcrop in the Gosau basin can be found in the *Riff von Unterbrein* (Reef of Unterbrein) near Russbach, which is stratigraphically positioned in the lower Hochmoos Formation (Wille-Janoschek, 1966; Höfling, 1985) according to Wagreich (1988). In this case, a patch reef of *Hippurites sulcatus* composes the actual barrier reef between a lagoonal milieu and the higher-

Profile W1			
Sample #	$\delta^{13}C$	$\delta^{18}O$	height cm
A 8	1.32	-1.88	636.0
A 9	1.20	-2.81	758.0
A 10	0.95	-3.09	808.0
A 11 Avg.	0.91	-2.79	919.0
A 12	0.32	-1.63	1020.0
A 13	1.53	-2.78	1120.0
A 14 Avg.	1.68	-2.12	1233.5
A 15 Avg.	1.28	-2.41	1293.5
A 16	1.46	-3.29	1320.5
A 17 Avg.	1.32	-4.83	1371.5
A 18 Avg.	1.12	-2.70	1409.5
A 19	1.61	-3.01	1467.5
A 20	1.61	-2.52	1506.5
A 21	0.54	-1.66	1539.5
A 22 Avg.	1.70	-2.86	1582.5
A 23 Avg.	0.93	-2.00	1649.5
A 24 End A	1.71	-2.41	1704.5
Profile E1			
B 1A Avg.	1.34	-3.19	150.0
B 1 B	1.63	-3.33	215.0
B 2	1.68	-2.62	405.0
B 3	1.12	-2.33	515.0
B 4	0.75	-2.55	725.0
B 5	1.80	-2.33	860.0
B 6 Avg.	1.07	-1.73	970.0
B 7	1.03	-3.42	1125.0
B 8	1.77	-3.21	1230.0
B 10	1.69	-2.89	1540.0
B 11	2.03	-2.56	1900.0
B 12 Avg.	2.10	-2.57	2060.0
B 13	1.83	-2.30	2220.0
B 14	1.96	-2.66	2488.0
B 15	2.14	-2.93	2723.0
B 16 Avg.	1.68	-2.76	3013.0
B 17	1.49	-3.35	3318.0
B 18 End B	1.78	-2.81	3603.0
Profile W1			
C 1	1.58	-2.60	130.0
C 2 Avg.	1.69	-2.36	260.0
C 3	1.84	-1.94	340.0
C 4	1.69	-2.21	450.0
C 5 Avg.	1.25	-2.27	545.5
C 6 End C	1.59	-2.00	652.0

Table 4: $\delta^{13}C$ and $\delta^{18}O$ values for all three profiles in Gosauschmied with height in profile indicated.

energy fore reef environment consisting of bioclastic limestone with large rudist fragments.

Other, much older occurrences of rudist-dominated depositional environments have been studied from the Gosau Group in the Lattengebirge, Germany, (Höfling, 1985), Brandenberg, Austria (Tyrol) (Sanders, 1997), Haidach, Austria (Tyrol) (Sanders and Baron-Szabo, 1997), Weisswasser, Austria (Lower Austria) (Sanders and Pons, 1999) and Gams, Austria (Styria) (Sanders and Pons, 1999). A common feature of these rudist-dominated occurrences of the LGS is a depositional environment from shoreface to inner shelf, with frequently a reef complex (biogenic or bioclastic) creating a lagoonal environment in the tidal to subtidal depths (often with radiolitid colonies) and mixed hippuritid, coral and radiolitid colonies beyond this area and extending to the inner open shelf. Depths do not attain neritic levels, and depositional morphology is flat to medium and most commonly some grade of carbonate ramp or shelf.

Hydrodynamic levels can vary greatly and have a substantial impact on the quantity and accumulation of bioclastic limestone, the quantity of rudist fragments in the sediments and also on the preservation of rudist biostromes in actual growth position.

5.2.2 Stratigraphic column of the Hochmoos Formation in Gosauschmied

Based upon the accumulated stratigraphic data and the overall facies distribution in the Hochmoos Formation at Gosauschmied together with the extent of each facies and the relevant structural data, a consolidated stratigraphic column can be constructed (see Fig. 15). This stratigraphic structure and the facies distribution allow for the development of deposition scenarios for the Hochmoos Formation in Gosauschmied, which follows in the next section (5.2.3).

5.2.3 Depositional Environment in Gosauschmied

Based upon the preceding analysis and discussion, the sedimentary evolution in Gosauschmied points towards a single 2nd order transgression/regression cycle on a medium-grade carbonate ramp or shelf setting exposed intermittently to high levels of hydrodynamic energy.

The relative sea-level variation is interpreted following the facies and microfacies evolution and the general interpretation of the environment. The succession starts (in the core of the anticline) with a mixed sandy/carbonate-lithic wacke and pebbly wacke with carbonate lithoclasts, indicating brackish to marginal marine environments (Wagreich, 1988) at a relative sea-level lowstand. Above this, profile W1 provides evidence of a transgression up to the inceptions of profile E1 and profile W2 and a first maximum flooding surface (MFS) at a relative highstand, at which point a parasequence in the area of the rudist biostromes is recorded, entailing a drop in relative sea-level to a range of several meters up to a maximum of 10m. This is then followed by a renewed transgression in which the marly limestone facies of upper profile W2 indicates a relative sea-level highstand and a second MFS. Above this, the growing inflow of terrigenous clasts up to the pebbly mudstone at the top of the ridge points toward a regressive half cycle to a relative lowstand below the uniform transgression of the marly, deeper neritic Bibereck Formation (Fig. 15). Furthermore,

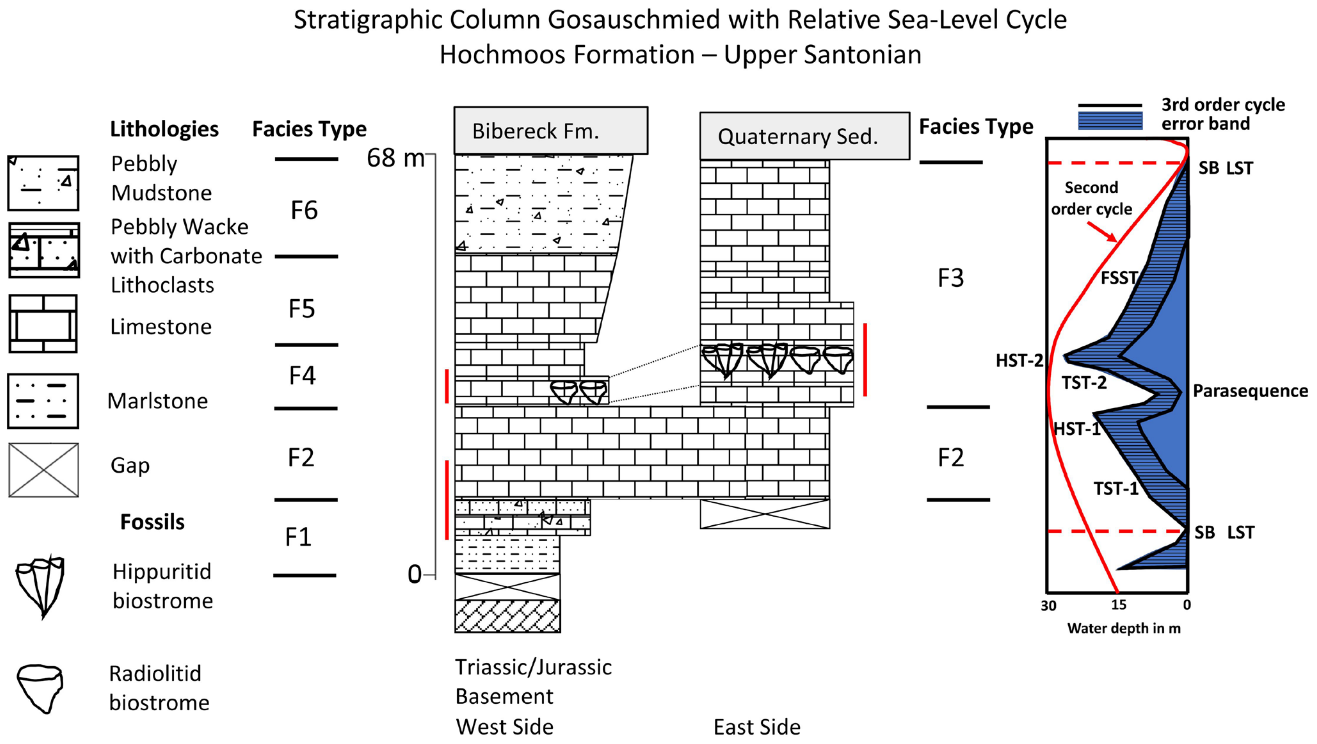

Figure 15: Consolidated stratigraphic column for the Hochmoos Formation at Gosauschmied with facies type. The red lines represent the profiles studied in-depth (W1 and W2 on the west side, E1 on the east side). Included on the right is the stratigraphic succession vs. relative sea level development in a single transgression-regression cycle (red curve, 2nd order). The black curve shows the 3rd order relative sea-level variation within the 2nd order cycle in the shelf area with an attendant error band to document potential sea-level range during the transgression-regression.

the synsedimentary tectonic activity of the Gosau basin (Wagreich and Decker, 2001) impacted significantly the succession and thickness of the sediments in this SE margin of the Gosau basin, introducing also tectonically-enhanced subsidence and thus water-depth variations.

Sanders and Pons (1999, p. 253, Fig. 3) provide a model for an idealized carbonate platform in an LGS shore-to-shelf setting. For the transgressive-regressive processes in Gosauschmied, this model has been slightly adapted to account for the facies succession in this particular area. The oldest stratigraphic beds in Gosauschmied show evidence of fluvial activity and terrestrial input, hence the beginning of the transgression occurs in an environment with an interplay of fluvial and marine (estuarine/delta) sedimentation developing from a relative sea-level lowstand. The entire depositional scenario is depicted in Figure 16, with a detailed description of each phase in the caption and discussion of the individual facies deposited in the transgression-regression cycle.

5.2.4 Sequence stratigraphy

The sequence depicted in Figure 16 serves as the basis for the sequence stratigraphic interpretation based on the presumed single 2nd order transgressive-regressive cycle in the Gosauschmied area. As discussed in the section on facies distribution in the study area, the stratigraphic succession can be reconstructed using facies types F1–F6.

Lowstand systems tract (LST) to transgressive systems tract (TST)

Stratigraphically, the Facies F1 sediments in the core of the anticline represent the oldest in the Hochmoos Formation at Gosauschmied. The marl interval at the center of the anticline contains high carbonate content, mollusc debris, a significant quantity of calcareous tests and scarce marine microfossils (foraminifera and ostracods). It is thus very probable that these marl sediments were deposited in a brackish estuarine milieu and represented the fluvially-dominated, coarse-grained lowstand deposits and an incipient transgression onto the Triassic-Jurassic basement of the NCA (see image 1 in Fig. 16).

When considering the mixed sandy/carbonate lithic and pebbly wacke that follow these marl sediments, there is an upward shoaling combined with an intermediate drop in relative sea-level: the carbonate lithoclasts of Dachstein limestone in the initial beds of profile W1 indicate that they arose from reworking of the substrate in a fluvial/marine environment similar to a fan delta. In the oldest beds of profile W1, there are only very limited fragments of Upper Cretaceous fossils. The high level of siliciclastic content further shows significant inflow of terrigenous material (detrital silica, reworked chert).

The mixed sandy/carbonate lithic and pebbly wacke from beds 1–7 in profile W1 provide a record of the transgression as it proceeded through the initial stages of a fan delta toward, ultimately, a first maximum flooding

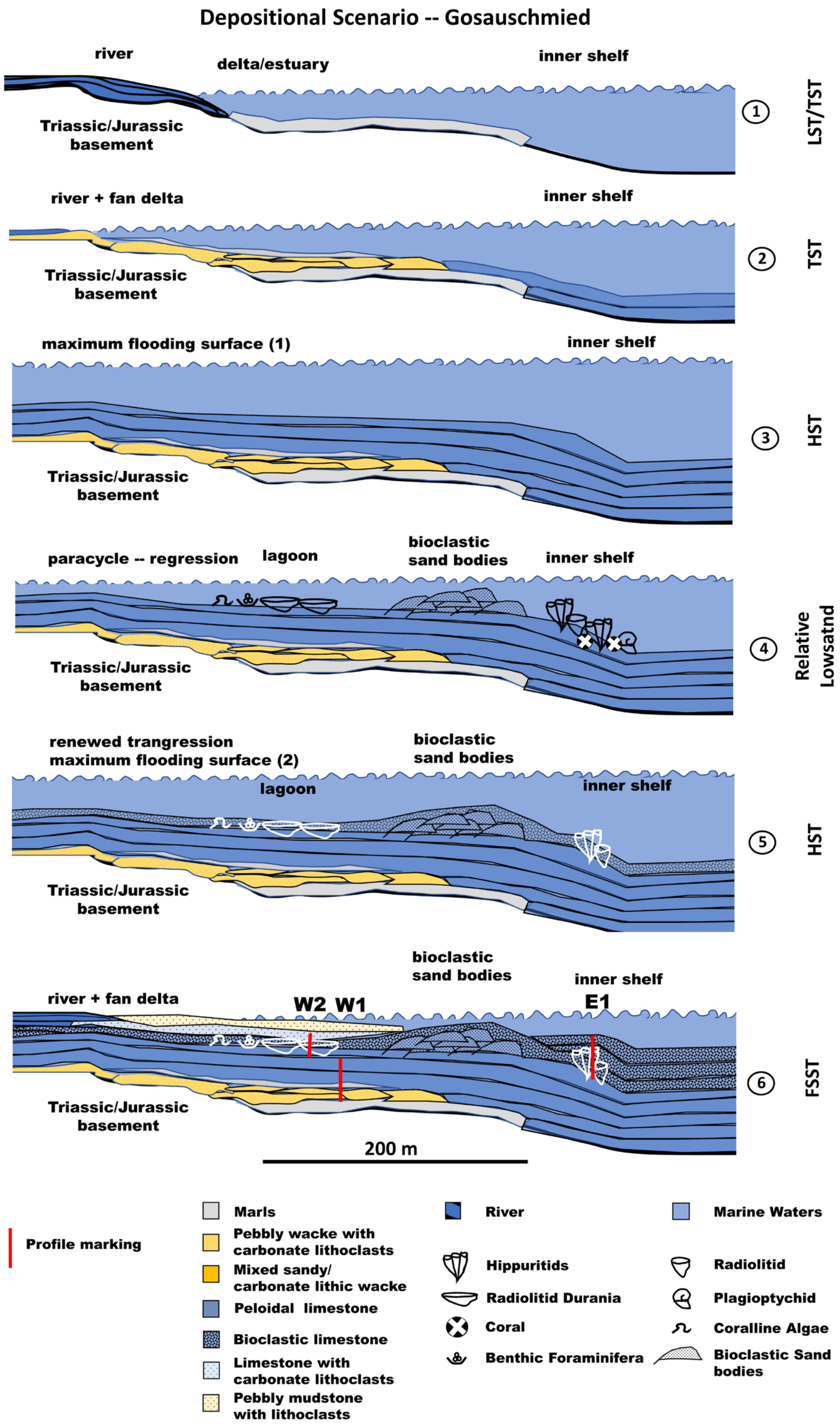

Figure 16: Description for each phase in the depositional scenario. 1. Beginning of the Transgressive Systems Tract (TST) from the Lowstand Systems Tract (LST) in an estuarine to fan-delta environment with a medium-grade inclination from shore to inner shelf at a relative sea-level lowstand. Bioclastic marls (F1) are laid down in an environment with significant fluvial inflow. 2. TST: mixed sandy/carbonate lithic and pebbly wacke (F1) accumulate in the proximal environment, while distal peloidal limestone is laid down in the inner shelf environment. Terrigenous clasts (sand, dolostones, pelsparite, carbonate lithoclasts) are intermixed with fragments of marine fossils and isolated foraminifera (miliolids, textularids). 3. Highstand Systems Tract (HST): peloidal limestone beds (F2) are laid down in a fully marine environment in progradational stacking patterns. Fossil content is low in uniform packstone to grainstone lithologies. A first relative MFS (Maximum Flooding Surface) is reached. 4. Relative stasis (minor lowstand): periodically calmer conditions allow for establishment of rudist colonies on both sides of the lagoonal barrier. Facies F3 sediments are on the open inner shelf, while Facies F4 sediments (beds 1 & 2 of Profile W2) are deposited in the lagoon. 5. HST: renewed transgression and a second MFS. In facies F4, marl content persists, while fossil content decreases. In facies F3 on the inner shelf, by contrast, significant beds of bioclastic limestone are deposited. 6. Falling Stage Systems Tract (FSST) to Lowstand: higher energy events lead to the accumulation of bioclastic sediments in the inner shelf (distal), while the proximal reworking of the shoreface leads to an inflow of terrigenous clasts in the lagoonal environment (F5 and F6). Return to high terrestrial/fluvial input in a fan delta environment in the proximal realm, while deeper areas continue to accumulate bioclastic limestone with large rudist fragments. The positions of profiles W1, W2 and E1 are marked in red.

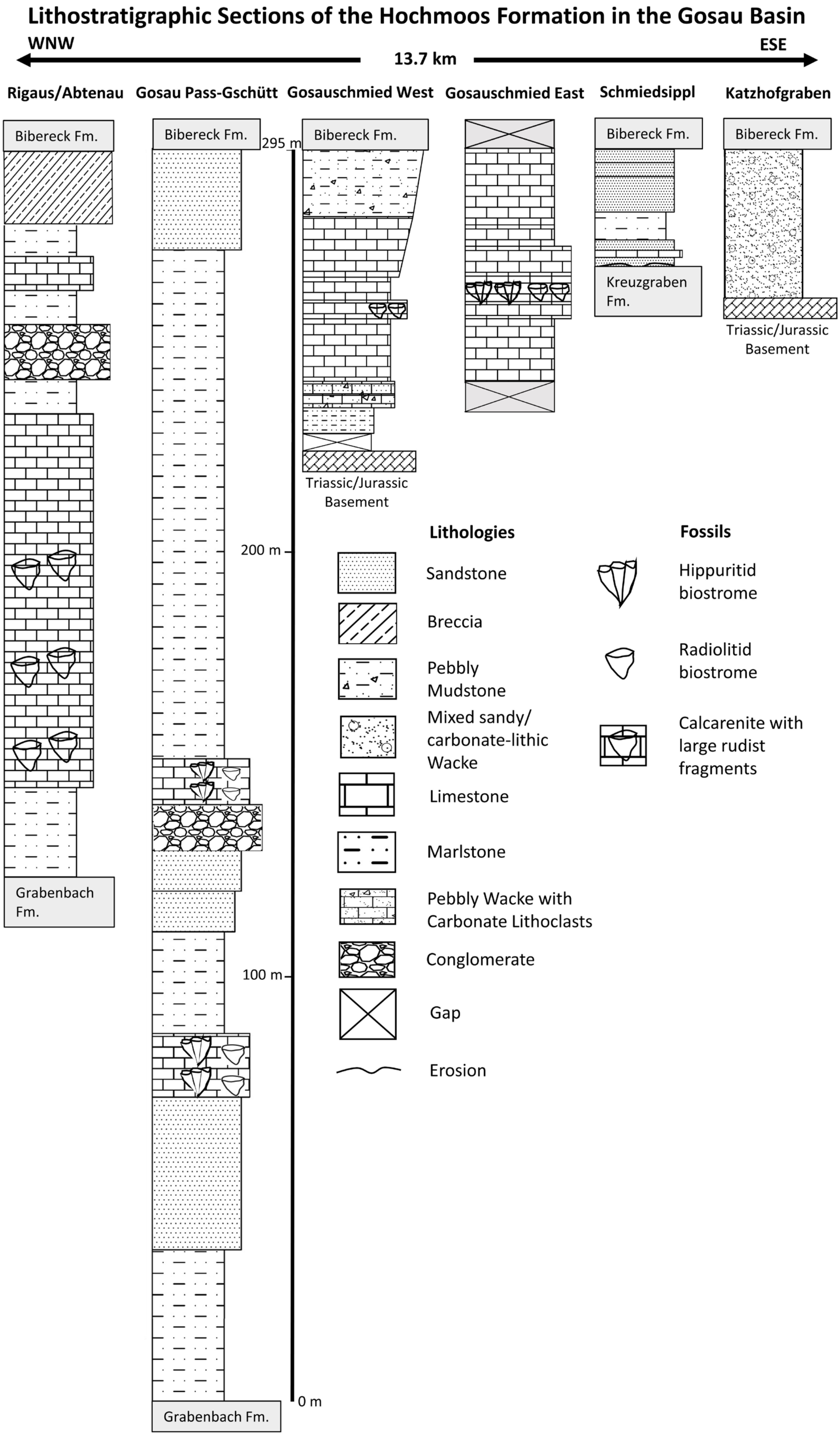

Figure 17: Comparison of the lithostratigraphic sections of six occurrences of the Hochmoos Formation in the Gosau/Rigaus area, including the legend of key lithologies and rudist biostromes.

surface (MFS) in the upper beds of the profile. Terrigenous clasts (sand, dolostones, pelsparite, carbonate lithoclasts) are intermixed with fragments of marine fossils and isolated foraminifera (miliolids, textulariids). The dolomitization beginning in bed 3 and complete in bed 4 most likely represents the result of evaporative processes in a marginal coastal and possibly intertidal area with intermittent flooding and receding waters at a relative lowstand. As the sea level rises again, calcarenite beds follow the pebbly carbonate-lithic wacke and contain chert, mono-crystalline quartz and carbonate sands, ultimately leading to a thin marl layer and the cessation of siliciclastic flow into the marine environment. Image 2 in Figure 16 depicts this transgressive scenario.

Highstand systems tract (HST)

The upper beds in profile W1 (9–24) represent a gradual transition to a fully marine environment with increasing peloidal content and decreasing marl content. This facies constitutes an extensive and foundational stratigraphic section in the Hochmoos Formation at Gosauschmied and is the result of distal carbonate beds being laid down in a coastal environment onto a medium-grade incline, ultimately leading to lagoonal and open shelf environments with reef structures in between.

Facies F2 rises beyond profile W1 and into the forest up the ridge, makes up most of the exposed outcrops between the highway and the brook (together with the pebbly wacke with carbonate lithoclasts in the anticline) and is to be found from top to bottom on both sides of the brook near the outlet of the dam. This is also the facies most prevalent on the surface throughout the study area and represents the hardest, most competent lithology (packstone to grainstone): a wide range of outcrops consist of this basic and undifferentiated peloidal limestone facies. In the stratigraphic column, facies F2 has an overall thickness ranging from 12 to 20 m. It underlies both profiles E1 and W2 and is hence older than both.

In profile W1, the fossil content in the first limestone beds appears to be of allochthonous origin, while the matrix itself gives evidence of bioturbation and firm-ground burrows. As of bed 14, there is barely any fossil content, and the matrix is unperturbed peloidal limestone. Image 3 in Figure 16 shows the carbonate sedimentation occurring during this TST.

Relative lowstand in the HST

The facies in profile E1 represents the transition from the more marginal W area to a fully and continuously marine milieu with significant biogenic and bioclastic production. During this phase of the transgressive/ regressive cycle, there is progradation of carbonate sediments and upward shoaling combined with a drop in sea-level to produce a relative lowstand after the first MFS. Rudist and coral-rudist colonies develop in self-protected to partially-protected environments, most likely in an inner shelf environment. The vast majority of sediments comprising facies F3 are bioclastic limestones with large rudist fragments that resulted from high energy events regularly destroying the established rudist and rudist-coral bio-assemblages and transporting the detritus in a parautochthonous manner into extensive skeletal mounds and beds. A series of prominent outcrops with only minimal macrofossil content, no apparent bedding and an extremely dense and competent limestone lithology to the west and north of profile E1 appear to represent bioclastic sand bodies at the seaward margin of a lagoonal milieu. The occurrence of sporadic rudist biostromes in beds 3 and 4 indicate that, at times, the environment was less exposed to storm events and allowed for a minimal preservation of some individual rudist colonies in growth position.

Facies F3 has strong similarities to the first two beds of profile W2: the fossil content is dominated by rudist and coral fragments that are heavily micritized; sparite fillings are common; and a brownish bioclastic marl sediment is frequently found in the chambers of the fossil fragments. One clear difference is that there are generally more benthic foraminifera in profile W2 than in E1. Furthermore, *Durania* sp. are found in profile W2; and, generally, radiolitid fragments are more numerous on the west side of the study area. Due to these similarities, the lower beds of profile W2 appear to be an extension of the depositional activity observed in profile E1 and most probably represent radiolitid colonies together with singular corals and benthic foraminifera in a partially-protected proximal lagoon environment shielded by the bioclastic sand bodies discussed above. The higher marl content in these lower beds of profile W2 would also indicate a less turbulent environment than in profile E1. In addition, radiolitid biostromes are more often observed in lagoonal environments, while hippuritid biostromes (often together with radiolitids) and corals are more commonly found in an open inner shelf milieu (Sanders and Pons, 1999). Finally, the presence of coralline algae fossils in profile W2 gives further support to this area being proximal vs. profile E1, where no such fossils could be identified. Image 4 in Figure 16 depicts this relative lowstand in the HST of the 2nd order transgressive-regressive cycle.

The lithology on both sides of the barrier in between indicates, however, that this environment was subjected to repeated high-energy events, producing the dominant bioclastic limestone of these two outcrops and their large rudist fragments. Beyond bed 4 in profile E1 and bed 1 in profile W2, there are no further intact biostromes and only rarely entire rudist fossils preserved in the outcrops.

HST

Subsequent to this relative lowstand, there is a renewed transgression leading to the upper sections of facies F4 with marly limestones and low fossil content, while also producing significant beds of bioclastic limestone in facies F3, as hydrodynamic energy levels increase. This second transgression and HST is depicted in image 5 of Figure 16.

Falling stage systems tract (FSST)
The incipient FSST in the transgressive/regressive cycle gives rise to facies F5. There is an increased inflow of terrestrial material in the proximal area from reworking of the shoreface as the waters recede, initially with only modest terrigenous clasts, while bioclastic limestone with rudist fragments continues to be deposited on the inner shelf.

LST
The final stage in the deposition of the Hochmoos Formation in Gosauschmied is the recurrence of a fan delta environment as the FSST progresses toward the final LST of the 2nd order cycle, resulting in the deposition of a pebbly mudstone with a clayey-silty matrix (image 6 in Fig. 16). In the proximal domain, this results in ever larger terrigenous clasts, while in the deeper distal realms, bioclastic limestone continues to accumulate.

With the termination of this cycle, sedimentation of the Hochmoos Formation concludes. On the west side of the study area, the neritic marls of the Bibereck Formation to the W and N overlie the Hochmoos Formation. It is presumed that the Bibereck sediments were laid down upon the entire Hochmoos Formation in the area, indicating the next major transgressive event (Wagreich, 1988).

5.3 Comparison with other occurrences of the Hochmoos Formation

The Gosau basin is known for its synsedimentary tectonic activity leading to varying thicknesses of sediments from the center of the basin to the margins (Wagreich and Decker, 2001). In light of this, six sections of the Hochmoos Formation were selected to compare the overall thicknesses of the outcrops in relation to their position in the basin center or at the margins (Fig. 1). These are positioned upon a WNW-ESE transect. Although presumed to have a common depositional history, Gosauschmied West and Gosauschmied East are shown separately.

Figure 17 shows the sedimentary columns of the six profiles of the Hochmoos Formation, indicating total thickness and basic lithology, including key biostromes if present (data collected from the following prior studies: Rigaus-Abtenau, Jarnik, 1994; Gosau Pass-Gschütt, Wagreich, 1988; Wagreich and Decker, 2001; Schmiedsippl, Wagreich and Neuhuber, 2005; Katzhofgraben, Trenkwalder, 1999). The distance from the far WNW margin at Rigaus-Abtenau to the far ESE margin at Katzhofgraben is approximately 13.7 km, a minimum extent for the Upper Cretaceous Gosau basin of the LGS (Wagreich and Decker, 2001).

These occurrences of the Hochmoos Formation are not only quite different with respect to thickness, but also were laid down in different stratigraphic contexts. In Rigaus-Abtenau and Gosau Pass-Gschütt, the Hochmoos Formation is underlain by the full succession of LGS formations (Kreuzgraben – Streiteck – Grabenbach), while in both Gosauschmied West and Katzhofgraben, it is presumed to be onlapping directly onto the Triassic-Jurassic basement (as carbonate lithoclasts of Dachstein limestone and other terrigenous clasts attest). The base of Gosauschmied East is less certain (as it lacks the Triassic/Jurassic terrigenous clasts), but is most likely also transgressing onto the Triassic-Jurassic basement. The Hochmoos Formation at Schmiedsippl, by contrast, was deposited (with an erosive surface) directly onto the Kreuzgraben Formation: it is presumed that either no sedimentation of the Grabenbach and Streiteck Formations occurred, or deposits from these two formations were subsequently fully eroded before the Hochmoos Formation sediments were deposited.

The Hochmoos Formation at Gosauschmied is further presumed to be an occurrence of the upper Hochmoos Formation (Wagreich, 1988; this study). The modest thickness, position at the SE margin of the basin and $^{87}Sr/^{86}Sr$ ratios all point to a temporal position in the uppermost Santonian directly at the boundary with the Campanian and potentially even crossing over into the Campanian in the youngest sediments.

Marls of the Bibereck Formation overlie each of the six occurrences except Gosauschmied East, which is covered by Quaternary deposits.

Wagreich and Decker (2001) show the effects of syntectonic activity in the Gosau area, delineating the effects of normal faults and strike-slip faults acting to create a pull-apart basin and effecting much higher sedimentation at the basin center and much more modest sedimentation at the basin margins. In Figure 18 (adapted from Wagreich and Decker, 2001), there is a schematic representation of the synsedimentary tectonic forces acting on the basin, which includes the approximate positions of the outcrops depicted in this comparison. This image shows the position and inclinations of the normal faults, indicating that the accommodation space for sedimentation increases dramatically toward the basin center and decreases toward the basin margins, particularly in the ESE corner of the basin, which includes Katzhofgraben, Schmiedsippl and Gosauschmied (West and East). This is reflected in the more modest sedimentation thickness of these outcrops compared to the major occurrence of the Hochmoos Formation at the basin center. The occurrence at Rigaus-Abtenau attains a thickness intermediate between those at the E-SE margin and Gosau Pass-Gschütt.

A crucial question regarding the transgression-regression cycle in the Hochmoos Formation in Gosauschmied relates to its causes and the interplay between relative sea-level rise and tectonic subsidence. Synsedimentary tectonic activity in the Gosau basin is responsible for dramatically varying thicknesses of the LGS occurrences, in general, and of the Hochmoos Formation, in particular, hence tectonic subsidence had a major impact on the magnitude of the accommodation space and the resulting sedimentary thickness. The succession of sediments in Gosauschmied, however, also points toward an overall relative sea-level

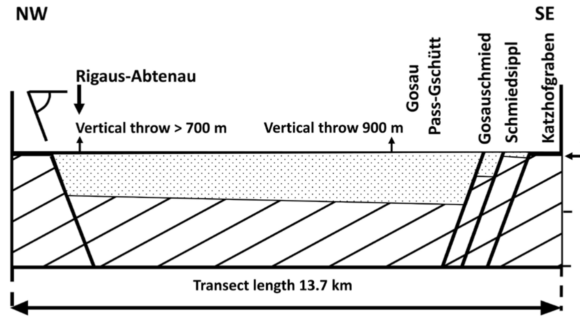

Figure 18: Schematic representation of synsedimentary normal fault activity and the approximate positions of the Hochmoos Formation outcrops in the Gosau basin (adapted from Wagreich and Decker, 2001). The hatched portion represents the basement, while the dotted section represents the accumulation of Gosau sediments.

cycle (2nd and 3rd orders) occurring in tandem with the tectonic subsidence: the sequence of fluvial-marine sandy/carbonate lithic wacke and calcarenites (F1) followed by fully marine peloidal limestones (F2) and bioclastic limestones (F3 and lower F4), ultimately leading again to peloidal limestones with carbonate lithoclasts (upper F4 and F5) and pebbly mudstone (F6) in the final stage, provides clear evidence of a relative sea-level rise and fall. Hence, the one process (relative sea-level rise and fall) overlies the more general and long-term process of tectonic subsidence occurring simultaneously, resulting in a tectonically-enhanced transgression-regression cycle. This may correlate to a major relative sea-level fall at the Santonian-Campanian boundary (Wolfgring et al., 2018), the KCa1 sequence boundary of Haq (2014). Considering that the relative sea-level cycle probably had a magnitude of approximately 30–40 m during the transgression-regression process in the shallow coastal shelf environment of the late Santonian, the attendant tectonic subsidence must have been in the range of 40–50 m to produce the overall thickness of 68 m in the Hochmoos Formation at Gosauschmied (accounting also for compaction and subsequent subaerial erosion of the sediments). The neritic marls of the Bibereck Formation which follow the Hochmoos Formation are, by contrast, almost exclusively the result of tectonic subsidence, as the Gosau basin rapidly descended through neritic to bathyal and abyssal depths in the Campanian (Wagreich, 1995).

6. Conclusions

The Hochmoos Formation at Gosauschmied along the former ESE margin of the extensional Gosau basin comprises a vertical succession of six facies types that, based on $^{87}Sr/^{86}Sr$ isotope ratios and carbon isotope excursion events, are interpreted as a late Santonian to possibly earliest Campanian transgressive-regressive cycle. The sediments cycle from marls, mixed sandy/carbonate-lithic wacke, pebbly wacke and calcarenites of estuarine and fan-delta milieus through normal-marine peloidal and bioclastic limestones to, finally, limestones with carbonate lithoclasts and pebbly mudstones with clasts of quartz of a fan delta that prograded during relative sea-level fall. The preponderance of bioclastic limestone with large rudist fragments on the east side of the study area and the sparse preservation of *in situ* rudist biostromes indicate impact of high-energy events (storms, tsunamis) that episodically destroyed the extant biostromes and heaped up the fragmented rudist shells into skeletal mounds on the inner shelf. Only rarely was the environment sufficiently calm for the preservation of rudists in growth position, as evidenced in profiles E1 and W2.

The maximum thickness of 68 m of the Hochmoos Formation at Gosauschmied renders it similar to other occurrences of the formation at the ESE margin of the Gosau basin (Schmiedsippl, Katzhofgraben), but considerably thinner than the nearly 300 m at Gosau Pass-Gschütt and the 170 m at Rigaus-Abtenau at the WNW basin margin. Along a WNW-ESE transect across the basin filling of Gosau, prior work (Wagreich and Decker, 2001) has documented synsedimentary normal faulting with a vertical throw of nearly 900 m at the basin center, declining to a mere 20–30 m at the ESE basin margin. We therefore conclude that the types, distribution and vertical successions of facies at Gosauschmied were driven by syndepositional tectonism. The relative sea-level cycle recorded in the upper part of the Hochmoos Formation is identified in most of the sections (Wagreich, 1988; Wagreich and Decker, 2001), and thus most probably relates to a tectonically-enhanced relative sea-level cycle around the Santonian-Campanian boundary.

References

Anderson, T.F., Arthur, M.A., 1983. Stable isotopes of oxygen and carbon and their application to sedimentologic and palaeoenvironmental problems. Stable Isotopes in Sedimentary Geology (SEMP Short Course) 10, 1–151.

Beauvais, M., 1982. Révision systématique des Madréporaires des couches de Gosau (Crétacé supérieur, Autriche), I.-V. Travaux du Laboratoire de paléontologie des invertébrés. Université Pierre et Marie Curie, 730 pp., Paris.

Bond, G. C., Kominz, M. A., 1984. Construction of tectonic subsidence curves for the early Paleozoic miogeocline, southern Rocky Mountains. Geological Society of America, Bulletin, 92, 155–173.

Brinkmann, R., 1934. Zur Schichtfolge und Lagerung der Gosau in den nördlichen Ostalpen. Sitzungsberichte der Preußischen Akademie der Wissenschaften, physikalisch-mathematische Klasse, 144, 145–149, Berlin.

Digitales Oberösterreichisches Raum-Informations-System [DORIS], https://doris.ooe.gv.at/default.aspx (accessed on 10 May 2021).

Dhondt, A. V., 1987. Bivalves from the Hochmoos Formation (Gosaugroup; Oberösterreich; Austria). Annalen des Naturhistorischen Museums in Wien, 88, 41–101.

Dunham, R.J., 1962. Classification of carbonate rocks according to depositional texture. In: Classification of Carbonate Rocks (Ed. W.E. Ham), American Association of Petroleum Geologists Memoir 1, 108–121.

Embry, A.F., Klovan, J.E., 1971. A late Devonian reef tract on northeastern Banks Island, N.W.T. Bulletin of Canadian Petroleum Geology, 19, 730–781.

Faupl, P., Wagreich, M., 1992. Cretaceous flysch and pelagic sequences of the Eastern Alps: correlations, heavy minerals, and paleogeographic implications. Cretaceous Research, 13, 387–403.

Faupl, P., Wagreich, M., 2000. Late Jurassic to Eocene palaeogeography and geodynamic evolution of the Eastern Alps. Mitteilungen der Österreichischen Geologischen Gesellschaft, 92, 79–94.

Flügel, E., 2004. Microfacies of Carbonate Rocks. 976 p., Springer-Verlag Berlin Heidelberg.

Folk, R.L., 1954. The distinction between grain size and mineral composition in sedimentary rock nomenclature. The Journal of Geology, 62, 344–359.

Folk, R.L., 1980. Petrology of Sedimentary Rocks. Austin, Texas, Hemphill Publishing Company, 182 pp.

Gili, E., Goetz, S., 2018. Part N, Volume 2, Chapter 26B: Paleoecology of rudists. Treatise Online 103, 1–29.

Haq, B.U., 2014. Cretaceous eustasy revisited. Global and Planetary Change, 113, 44–58. https://doi.org/10.1016/j.gloplacha.2013.12.007

Höfling, R., 1985. Faziesverteilung und Fossilvergesellschaftungen im karbonatischen Flachwasser-Milieu der alpinen Oberkreide (Gosau-Formation). Münchner Geowissenschaftliche Abhandlungen, A, 3, 241 pp.

Jarnik, M., 1994. Zur Sedimentologie, Stratigraphie und Tektonik der Gosau Rigaus-Abtenau (Salzburg, Österreich), Wien, Universität, Diplomarbeit, UB Wien, unpublished thesis.

Jarvis, I., Mabrouk, A., Moody, R.T. J., De Cabrera, S.C., 2002. Late Cretaceous (Campanian) carbon isotope events, sea-level change and correlation of the Tethyan and Boreal realms. Palaeogeography, Palaeoclimatology, Palaeoecology 188, 215–248. https://doi.org/10.1016/S0031-0182(02)00578-3

Jarvis, I., Gale, A.S., Jenkyns, H.C., Pearce, M.A., 2006. Secular variation in Late Cretaceous carbon isotopes: a new δ13C carbonate reference curve for the Cenomanian–Campanian (99.6–70.6 Ma). Geological Magazine 143, 561–608. https://doi.org/10.1017/S0016756806002421

Kearney, K., 2020. Stratigraphic Analysis of Marine Carbonates in the Hochmoos Formation (upper Santonian) in Gosauschmied, Upper Austria. Unpublished Master's thesis, University of Vienna, 153 pp. https://utheses.univie.ac.at/detail/54869#, https://doi.org/10.25365/thesis.62066

Kollmann, H. A., 1982. Gosauablagerungen im Becken von Gosau. In: Plöchinger, B., Erläuterungen zu Blatt 95 St. Wolfgang im Salzkammergut, 30–34, Wien 1982.

Kollmann, H.A., Summesberger, H., 1982. Excursions to Coniacian - Maastrichtian in the Austrian Alps. Exkursionsführer Fourth Meeting Working Group Coniacian – Maastrichtian Stages, 105 pp., Wien 1982.

Lahodynsky, R., 1981. Bericht 1978 über geologische Aufnahme im Kreide-Tertiärbecken von Gosau auf Blatt 95 St. Wolfgang. Verhandlungen der Geologischen Bundesanstalt, 1979, A 109–110.

Lahodynsky, R., 1983. Bericht 1979 über geologische Aufnahme in der flyschartigen Gosau Blatt 95 St. Wolfgang. Verhandlungen der Geologischen Bundesanstalt, 1980, 68–69.

Lahodynsky, R., 1988. Lithostratigraphy and sedimentology across the Cretaceous/Tertiary boundary in the Flyschgosau (Eastern Alps, Austria). Revista Española de Paleontología Extraordinario 73–82.

Lill von Lilienbach, K., 1830. Ein Durchschnitt aus den Alpen mit Hindeutungen auf die Karpathen. Leonhard und Bronns Jahrbuch, Heidelberg.

McArthur, J.M., Howarth, R. J., Bailey, T.R., 2001. Strontium isotope stratigraphy: LOWESS Version 3: best fit to the marine Sr-isotope curve for 0–509 Ma and accompanying look-up table for deriving numerical age. Journal of Geology 109, 155–170. https://doi.org/10.1086/319243

Neuhuber, S., Gier, S., Hohenegger, J., Wolfgring, E., Spoetl, C., Strauss, P., Wagreich, M., 2016. Palaeoenvironmental changes in the northwestern Tethys during the Late Campanian Radotruncana calcarata Zone: Implications from stable isotopes and geochemistry. Chemical Geology 420, 280–296. https://doi.org/10.1016/j.chemgeo.2015.11.023

Pettijohn, F.J., Potter, P.E., Siever, R., 1973. Sand and sandstone. Springer, New York, 618 pp.

Plöchinger, B., 1982. Geologische Karte der Republik Österreich, 095 St. Wolfgang im Salzkammergut, 1:50:000. Geologische Bundesanstalt, Wien.

Pohl, A., Donnadier, Y., Godderis, Y., Lanteaume, C., Hairabian, A., Frau, C., Micheh, J., Laugie, M., Reijmer, J.J.G., Scotese, C.R., Borgomano, J., 2020. Carbonate platform production during the Cretaceous. GSA Bulletin v. 132; no. 11/12; p. 2606–2610; https://doi.org/10.1130/B35680.1

Preisinger, A., Zobetz, E., Gratz, A., Lahodynsky, R., Becke, M., Mauritsch, H.J., Eder, G., Grass, F., Rögl, F., Stradner, H., Surenian, R., 1986. The Cretaceous/Tertiary boundary in the Gosau Basin, Austria. Nature 322, 797–799.

Reuss, A.E., 1854. Beiträge zur Charakteristik der Kreideschichten der Ostalpen, besonders im Gosauthale und am Wolfgangsee. Denkschrift der Österreichischen Akademie der Wissenschaften, mathematisch-naturwissenschaftlichen Klasse, Bd. 7, 156 pp.

Sanders, D., 1997. Upper Cretaceous Transgressive Shore Zone Deposits ("Untersberger Marmor" Auct.) in the Eastern Part of the Tyrol (Austria): An Overview: Geologische Paläontologische Mitteilungen Innsbruck, 22, 101–121.

Sanders, D., 1998. Tectonically controlled late Cretaceous terrestrial to neritic deposition (Northern Calcareous Alps, Tyrol, Austria). Facies, 39, 139–179.

Sanders, D., Baron-Szabo, R. C., 1997. Coral-Rudist Bioconstructions in the Upper Cretaceous Haidach

Section (Gosau Group; Northern Calcareous Alps, Austria). Facies, 36, 69–90.

Sanders, D., Höfling, R., 2000. Carbonate deposition in mixed siliciclastic-carbonate environments on top of an orogenic wedge (Late Cretaceous, Northern Calcareous Alps, Austria): Sedimentary Geology, 137, 127–146. https://doi.org/10.1016/S0037-0738(00)00084-1

Sanders, D., Pons, J. M., 1999. Rudist formations in mixed siliciclastic-carbonate positional environments, Upper Cretaceous, Austria: stratigraphy, sedimentology, and models of development. Palaeogeography, Palaeoclimatology, Palaeoecology, 148, 249–284. https://doi.org/10.1016/S0031-0182(98)00186-2

Schlagintweit, F., 1992. Benthonische Foraminiferen aus Flachwasserkarbonaten der Oberkreide der Nördlichen Kalkalpen (Gosauschichtgruppe, Österreich). Mitteilungen der Österreichischen Geologischen Gesellschaft, 84, 327–353.

Skelton, P.W., 2013. Rudist classification for the revised Bivalvia volumes of the 'Treatise on Invertebrate Paleontology.' Caribbean Journal of Earth Science, 45, 9–33.

Spötl, C., Vennemann, T., 2003. Continuous-flow isotope ratio mass spectrometric analysis of carbonate minerals. Rapid Communications in Mass Spectrometry, 17, 1004–1006. https://doi.org/10.1002/rcm.1010

Steuber, T., 2004. Turonian-Campanian Plagioptychidae (Mollusca: Hippuritoidea) of Gosau-type rudist formations of the Alps (Austria), Annalen des Naturhistorischen Museums Wien, 106/A, 103–121.

Summesberger, H., 1979. Eine obersantone Ammonitenfauna aus dem Becken von Gosau (Oberösterreich). Annalen des Naturhistorischen Museums Wien, 82, 109–176.

Summesberger, H., 1985. Ammonite zonation of the Gosau Group (Upper Cretaceous, Austria). Annalen des Naturhistorischen Museums Wien, 87, 145–166.

Summesberger, H., Kennedy, W.J., 1996. Turonian ammonites from the Gosau Group (Upper Cretaceous; Northern Calcareous Alps; Austria) with a revision of Barroisiceras haberfellneri (Hauer, 1866). Beiträge zur Paläontologie, 21, 105–177.

Summesberger, H., Kennedy, W. J., Wolfgring, E., Wagreich, M., Tröger, K.A., Skoumal, P., 2017. Integrated stratigraphy of the upper Santonian (Upper Cretaceous) Hochmoos and Bibereck Formations of the Schattaugraben section (Gosau Group; Northern Calcareous Alps, Austria). Abhandlungen der Geologischen Bundesanstalt, 71, 151–248.

Thibault, N., Jarvis, I., Voigt, S., Gale, A.S., Attree, K., Jenkyns, H.C., 2016. Astronomical calibration and global correlation of the Santonian (Cretaceous) based on the marine carbon isotope record. Paleoceanography, 31, 847–865. https://doi.org/10.1002/2016PA002941

Trenkwalder, M., 1999. Stratigraphie, Tektonik und Mikrofauna der Oberen Kreide südlich von Gosau. Unpublished Diplomarbeit, University of Innsbruck, 154 pp.

Tröger K.A.; Summesberger, H., 1994. Coniacian and Santonian inoceramid bivalves from the Gosau-Group (Cretaceous, Austria) and their biostratigraphic and palaeobiogeographic significance. Annalen des Naturhistorischen Museums in Wien, 96A, 161–197.

Wagreich, M., 1986. Sedimentologische und stratigraphische Untersuchungen des tieferen Abschnittes der Gosauschichten von Gosau und Russbach (Oberösterreich – Salzburg). Unpublished doctoral thesis at the Faculty of Formal and Natural Sciences at the University of Vienna, Austria, 239 pp.

Wagreich, M., 1988. Sedimentologie und Beckenentwicklung des tieferen Abschnittes (Santon-Untercampan) der Gosauschichtgruppe von Gosau und Rußbach (Oberösterreich - Salzburg), Jahresbuch der Geologischen Bundesanstalt, 131, 663–685.

Wagreich, M., 1991. Subsidenzanalyse an kalkalpinen Oberkreideserien der Gosaugruppe (Österreich). Zentralblatt für Geolologie und Paläontologie, Teil 1, 1645–1657.

Wagreich, M., 1992. Correlation of Late Cretaceous calcareous nannofossil zones with ammonite zones and planktonic foraminifera: The Austrian Gosau sections. Cretaceous Research, 13, 505–516.

Wagreich, M., 1995. Subduction tectonic erosion and Late Cretaceous subsidence along the northern Austroalpine margin (Eastern Alps, Austria). Tectonophysics, 242, 63–78.

Wagreich, M., 1998. Lithostratigraphie, Fazies und Sequenzstratigraphie der Gosau Gruppe von Bad Ischl und Strobl am Wolfgangsee (Oberturon-Maastricht, Nördliche Kalkalpen, Österreich). Jahresbuch der Geologischen Bundesanstalt, 141, 209–234.

Wagreich, M., 2003. Die Entwicklung des Gosaubeckens Während der Kreidezeit/The Evolution of the Gosau Basin During the Cretaceous, in Weidinger, J.T, Lobitzer, H., Spitzbart, I. (Hrsg.) 2003. Beiträge zur Geologie des Salzkammerguts, Gmundner Geo-Studien 2 Erkudok, Institut Museum Gmunden, pp. 21–28.

Wagreich, M., Krenmayr, H.G., 1993. Nannofossil biostratigraphy of the Late Cretaceous Nierental Formation, Northern Calcareous Alps (Bavaria, Austria). Zitteliana 20, 67–77.

Wagreich, M., Faupl, P., 1994. Paleogeography and geodynamic evolution of the Gosau Group of the Northern Calcareous Alps (Late Cretaceous, Eastern Alps, Austria). Palaeogeography, Palaeoclimatology, Palaeoecology, 110, 235–254. https://doi.org/10.1016/0031-0182(94)90086-8

Wagreich, M., Decker, K., 2001. Sedimentary tectonics modelling of the type Upper Cretaceous Gosau basin (Northern Calcareous Alps, Austria). International Journal of Earth Sciences, 90, 714–726. https://doi.org/10.1007/s005310000181

Wagreich, M., Hohenegger, J., Neuhuber, S., 2012. Nannofossil biostratigraphy, strontium and carbon isotope stratigraphy, cyclostratigraphy and an astronomically calibrated duration of the Late

Campanian Radotruncana calcarata Zone. Cretaceous Research, 38, 80–96. https://doi.org/10.1016/j.cretres.2012.04.006
Wagreich, M., Neuhuber, S., 2005. Stratigraphy and geochemistry of an Early Campanian deepening succession (Bibereck Formation, Gosau Group, Austria). Earth Science Frontiers, 12, 123–131.
Wagreich, M., Lukeneder, A., Egger, H., 2008. Cretaceous History of Austria. Berichte der Geologischen Bundesanstalt, 74, 12–30.
Wagreich, M., Summesberger, H., Kroh, A., 2010. Late Santonian bioevents in the Schattau section, Gosau Group of Austria – implications for the Santonian–Campanian boundary stratigraphy. Cretaceous Research 31, 181–191. https://doi.org/10.1016/j.cretres.2009.10.003
Weigel, O., 1937. Stratigraphie und Tektonik des Beckens von Gosau. Jahrbuch der Geologischen Bundesanstalt, 87, 11–40.
Weiss, W., 1975. Mikropaläontologische Gliederung der Unteren Gosauschichten im N-Teil des Beckens von Gosau (Oberösterreich). Unpublished Diplomarbeit Universität Tübingen, 73 S., Tübingen.
Weiss, W., 1977. Korrelation küstennaher und küstenferner Faziesbereiche in den Unteren Gosauschichten (Oberkreide, Österreich). Neues Jahrbuch für Geologie und Paläontologie, Monatshefte, 1977, 289–302.
Wille-Janoschek, U., 1966. Stratigraphie und Tektonik der Schichten der Oberkreide und des Alttertiärs im Raume von Gosau und Abtenau (Salzburg). Jahrbuch der Geologischen Bundesanstalt, 109, 91–172.
Wolfgring, E., Wagreich, M., Dinarès-Turell, J., Gier, S., Böhm, K., Sames, B., Spötl, C., Popp, F., 2018. The Santonian–Campanian boundary and the end of the Long Cretaceous Normal Polarity-Chron: Isotope and plankton stratigraphy of a pelagic reference section in the NW Tethys (Austria). Newsletters on Stratigraphy, 51/4, 445–476. https://doi.org/10.1127/nos/2018/0392
Wright, V.P., 1992: A revised classification of limestones. Sedimentary Geology, 76, 177–185. https://doi.org/10.1016/0037-0738(92)90082-3
Zakharov, Y.D., Kakabadze, M.V., Sharikadze, M.Z., Smyshlyeva, O.P., Sobolev, E.S., Safronov, P.P., 2018. The stable O- and C-isotope record of fossils from the upper Barremian–lower Albian of the Caucasus–palaeoenvironmental implications. Cretaceous Research, 87, 55–73. https://doi.org/10.1016/j.cretres.2017.07.023
Zekeli, F., 1852. Die Gastropoden der Gosaugebilde. Abhandlungen der Geologischen Reichsanstalt, 1, 124 pp.
Ziegler, P.A., 1988. Evolution of the Arctic-North Atlantic of the Western Tethys. American Association of Petroleum Geologists, Memoir 43, 198 pp.
Zittel, F., 1866. Die Bivalven der Gosaugebilde in den nordöstlichen Alpen. Beitrag zur Charakteristik der Kreideformation in Österreich. Denkschriften der Kaiserlich-königlichen Akademie der Wissenschaften, mathematisch- naturwissenschaftliche Klasse, 26, 1–122.
Zuffa, G.G., 1985. Optical analyses of arenites: Influence of methodology on compositional results. In: Zuffa, G.G. (ed.), Provenance of Arenites, 165–189. NATO Advanced Science Institute Series, D. Reidel Publishing Company, Dordrecht, 408 pp.

Received: 20.12.2021
Accepted: 3.5.2022
Editorial Handling: Björn Berning

Zeitschrift/Journal: Austrian Journal of Earth Sciences

Jahr/Year: 2022

Band/Volume: 115

Autor(en)/Author(s): Kearney Kevin, Wagreich Michael, Sanders Diethard

Artikel/Article: Stratigraphic architecture of a mixed clastic-carbonate succession and 87Sr/86Sr-based chronostratigraphy along the margin of a synorogenic extensional basin (Hochmoos Formation, upper Santonian, Northern Calcareous Alps) 74-99